Methane activation by cobalt cluster cations, Co_n^+ (n=2–16): Reaction mechanisms and thermochemistry of cluster-CH_x (x=0–3) complexes

Murat Citir, Fuyi Liu,[a] and P. B. Armentrout[b]
Department of Chemistry, University of Utah, Salt Lake City, Utah 84112, USA

(Received 19 November 2008; accepted 5 January 2009; published online 5 February 2009)

The kinetic energy dependences of the reactions of Co_n^+ (n=2–16) with CD_4 are studied in a guided ion beam tandem mass spectrometer over the energy range of 0–10 eV. The main products are hydride formation, Co_nD^+, dehydrogenation to form $Co_nCD_2^+$, and double dehydrogenation yielding Co_nC^+. These primary products decompose to form secondary and higher order products, Co_nCD^+, $Co_{n-1}D^+$, $Co_{n-1}C^+$, $Co_{n-1}CD^+$, and $Co_{n-1}CD_2^+$ at higher energies. Adduct formation of $Co_nCD_4^+$ is also observed for the largest cluster cations, $n \geq 10$. In general, the efficiencies of the single and double dehydrogenation processes increase with cluster size, although the hexamer cation shows a reduced reactivity compared to its neighbors. All reactions exhibit thresholds, and cross sections for the various primary and secondary reactions are analyzed to yield reaction thresholds from which bond energies for cobalt cluster cations to D, C, CD, CD_2, and CD_3 are determined. The relative magnitudes of these bond energies are consistent with simple bond order considerations. Bond energies for larger clusters rapidly reach relatively constant values, which are used to estimate the chemisorption energies of the C, CD, CD_2, and CD_3 molecular fragments to cobalt surfaces. © *2009 American Institute of Physics*. [DOI: 10.1063/1.3073886]

I. INTRODUCTION

Transition metal clusters have been extensively investigated over the past two decades, in part because clusters may serve as effective and experimentally tractable models for surfaces and heterogeneous catalysts. In addition, cluster research serves as an ideal interface between experimental and theoretical studies. The size dependence of cluster reactivities is a fascinating and intriguing issue and has attracted much attention both theoretically and experimentally.[1–3] Our group has measured bond energies for transition metal cluster-ligand complexes[4–16] using guided ion beam tandem mass spectrometry. Surprisingly, these thermochemical values rapidly reach plateaus that are comparable to similar quantities for metal surfaces, when available. For example, in the $Co_n^+ + D_2$ reaction system,[17] Co_n^+–D bond energies reach a relatively constant value of about 2.59 ± 0.10 eV for $n \geq 10$. This is close to the bulk-phase value for hydrogen binding to bulk cobalt surfaces, about 2.63 eV for measurements on Co(0001) (Refs. 18 and 19) and Co(10$\bar{1}$0) (Ref. 20) surfaces. Likewise a range of calorimetry measurements indicate that oxygen atoms bind to bulk cobalt surfaces with strengths of 4.7–5.1 eV,[21–24] which agrees with our measurements of $D(Co_n^+–O) = 4.7 \pm 0.2$ eV (n=3–19) and $D(Co_n^+–2O)/2 = 5.1 \pm 0.3$ eV (n=4–18).[25]

In contrast to these atomic adsorbates, similar bulk-phase thermochemistry is not readily available for molecular adsorbates. However, in studies of the $Fe_n^+ + CD_4$ (Ref. 11) and $Ni_n^+ + CD_4$ (Ref. 26) reaction systems, we find that bond energies for these metal cluster cations to the molecular fragment CD and CD_2 also reach plateaus for modest sized clusters, $n \geq 10$. In the case of Fe_n^+, these cluster bond energies are 5.9 ± 0.4 and 4.2 ± 0.4 eV, respectively,[11] in reasonable agreement with values of 6.2 and 4.5 eV, respectively, estimated using a bond order conservation-Morse potential approach for binding to Fe/W(110) surfaces.[21] Also, recommended bond energies for Ni_n^+ to CD and CD_2 (5.9 ± 0.2 and $\geq 3.9 \pm 0.1$ eV, respectively) are in good agreement with estimated revisions of *ab initio* calculations of the chemisorption energies of CH and CH_2 on Ni(111).[27] Overall, these comparisons suggest that the cluster-surface analogy provides relevant thermodynamic information for surface science and catalysis.

The reaction of hydrocarbon fragments on catalytically active transition metal surfaces has been extensively studied because of the commercial importance of hydrocarbon formation reactions. Catalytic reactions, such as Fischer–Tropsch (FT), methane partial oxidation, fuel reforming, water gas shift, steam reforming, and hydrocarbon processing, involve the binding of molecular fragments to surfaces. It is believed that methyl (CH_3), methylidene (CH_2), and methylidyne (CH) groups are important intermediates in many of these catalytic reactions, but the thermodynamic data for such bulk-phase systems are quite sparse. In addition to these molecular fragments, the interaction of atomic carbon with cobalt surfaces is extremely important in many of these catalytic systems, particularly in FT synthesis. In the FT reaction, CO and H_2 are catalytically converted into hydrocarbons, thereby producing clean transportation fuels from non-crude-oil feedstocks.[28–32] Such carbon monoxide hydrogenation reactions have been studied on Co(0001), Co(11$\bar{2}$0), and Co(10$\bar{1}$2),[33] and on Co/W(100) and Co/W(110),[34] Co/Al_2O_3,[35–38] and Co foils and Co/Au surface.[39] Activation

[a]Present address: National Synchrotron Radiation Laboratory, University of Science and Technology of China, Hefei, China.
[b]Electronic mail: armentrout@chem.utah.edu.

energies for methane formation ranging from 86 to 150 kJ/mol have been reported and are likely attributable to the CO activation step. Again little information is available for the binding of carbon to cobalt surfaces, although Benziger[21] estimated this value from the enthalpy of formation of bulk compounds.

In the present study, we investigate the reactions of size-selected cobalt cluster cations (2–16 atoms) with methane using guided ion beam tandem mass spectrometry. By measuring and analyzing the kinetic energy dependence of the reaction products from thermal energies to approximately 10 eV, we are able to determine threshold energies for a number of processes and obtain bond energies for the deuterated analogs of the hydrocarbon molecular fragments, CH, CH_2, and CH_3, to size-specific cobalt cluster cations. This investigation gives insight into C–H bond activation on cobalt surfaces and provides quantitative thermodynamic information regarding the intermediates and products formed in these reactions. This thermodynamic information is compared to available theoretical estimates as no bulk-phase experimental values presently exist.

II. EXPERIMENTAL SECTION

The ion beam apparatus used in this study has been described in detail previously.[40] A more general overview of the apparatus is given here. Cobalt cluster cations are produced in a water-cooled laser ablation source. The output of a copper vapor laser (Oxford ACL 35) operating at 7–8 kHz repetition rate is tightly focused onto a rotating and translating cobalt rod inside an aluminum source block. The copper vapor laser produces 3–4 mJ per pulse at 511 and 578 nm. The ablated ions are entrained in a continuous flow of He passing at a flow rate between $(4-6)\times10^3$ SCCM (SCCM denotes cubic centimeters per minute at STP). The cobalt clusters ions are formed in a 2 mm diameter $\times$ 63 mm long tube that immediately follows the source block. The gas mixture then undergoes a mild supersonic expansion in a field-free region that further cools the internal modes of the clusters. Previous studies have shown that the clusters are likely to be near room temperature and not internally excited.[41–43]

Positively charged cobalt clusters are extracted from the ion source, accelerated, focused, and injected into a 60° magnetic sector momentum analyzer. The mass selected ions are decelerated to a selected kinetic energy and focused into a radio-frequency (rf) octopole ion guide.[44,45] Reactions take place within the octopole where the neutral gas CD_4 is introduced into a reaction cell. The pressure of CD_4 (99.8% purity) in the reaction cell is kept relatively low to reduce the probability of multiple collisions with the ions. All products reported here are the result of single bimolecular encounters between the reactants, as confirmed by pressure dependence studies at 0.2 and 0.4 mTorr of CD_4. The octopole guide is biased with dc and rf voltages. The dc voltage allows accurate control of the translational energy of the reactant ions. The rf electric field establishes a potential well to trap ions in the radial direction without affecting their axial energy, and thus allows efficient collection of all fragment ions and transmitted parent cluster ions. These ions drift out of the collision chamber to the end of the octopole, where they are extracted and injected into a quadrupole mass filter for mass analysis. Finally, the ion intensities are measured with a Daly detector[46] coupled with standard pulse counting techniques. Reactant ion intensities used in these studies ranged from $(1-8)\times10^5$ ions/s. Conversion of observed product-ion intensities into absolute reaction cross sections is accomplished as discussed in detail previously.[47] Absolute errors in the cross sections are estimated as $\pm30\%$.

Data collection for each reaction system was repeated several times to ensure reproducibility of results. Collision-induced dissociation (CID) experiments with Xe were performed on all the cluster ions to verify their identity and the absence of any excessive internal excitation. In all instances, CID thresholds are consistent with those previously reported.[41] Laboratory ion energies (laboratory) are converted to energies in the center-of-mass (CM) frame using the stationary target approximation, $E(\mathrm{CM})=E(\mathrm{lab})\times m/(m+M)$, where m and M are the masses of the neutral and ionic reactants, respectively.[47] All energies reported below are in the CM frame unless otherwise noted. The absolute zero and distribution of the ion kinetic energies were determined using the octopole as a retarding energy analyzer. The distribution of ion kinetic energies varies with cluster size from 0.7 to 2.0 eV (laboratory) in these experiments. The uncertainty in the absolute energy scale is 0.05 eV in the laboratory frame.

III. RESULTS

Cobalt cluster cations, Co_n^+ ($n=2-16$), were reacted with CD_4 as a function kinetic energy over a range of thermal to about 10 eV in the CM frame. Deuterated methane was used to enhance the mass separation between products. Results for selected cobalt cluster cations reacting with CD_4 are shown below with results for the remaining clusters provided in the supplemental figures.[48] The observed reactions are organized in the following manner. Reactions (1)–(5) comprise a group in which no loss of cobalt atoms occurs,

$$\mathrm{Co}_n^+ + \mathrm{CD}_4 \rightarrow \mathrm{Co}_n\mathrm{D}^+ + \mathrm{CD}_3 \quad (1)$$

$$\rightarrow \mathrm{Co}_n\mathrm{C}^+ + 2\mathrm{D}_2 \quad (2)$$

$$\rightarrow \mathrm{Co}_n\mathrm{CD}^+ + \mathrm{D} + \mathrm{D}_2 \quad (3)$$

$$\rightarrow \mathrm{Co}_n\mathrm{CD}_2^+ + \mathrm{D}_2 \quad (4)$$

$$\rightarrow \mathrm{Co}_n\mathrm{CD}_3^+ + \mathrm{D}. \quad (5)$$

The second group includes reactions (6)–(10) that are observed at higher energies. In these processes, products containing fewer cobalt atoms are formed as a result of dissociation of the product ions formed in reactions (1)–(5),

$$\mathrm{Co}_n^+ + \mathrm{CD}_4 \rightarrow \mathrm{Co}_{n-1}\mathrm{D}^+ + [\mathrm{Co} + \mathrm{CD}_3] \quad (6)$$

$$\rightarrow \mathrm{Co}_{n-1}\mathrm{C}^+ + \mathrm{Co} + 2\mathrm{D}_2 \quad (7)$$

$$\rightarrow \mathrm{Co}_{n-1}\mathrm{CD}^+ + [\mathrm{Co} + \mathrm{D}] + \mathrm{D}_2 \quad (8)$$

$$\rightarrow \mathrm{Co}_{n-1}\mathrm{CD}_2^+ + \mathrm{Co} + \mathrm{D}_2 \quad (9)$$

$$\rightarrow Co_{n-1}CD_3^+ + [Co + D], \quad (10)$$

where brackets indicate the possibility that the products shown are covalently bound. The last group includes the simple CID reaction (11),

$$Co_n^+ + CD_4 \rightarrow Co_{n-1}^+ + Co + CD_4. \quad (11)$$

Generally, the identity of the associated neutral products is clear, but in reactions (6), (8), and (10), there are two possible pathways. Identification of the observed pathways depends on thermodynamic arguments, as discussed below. For reactions (8) and (10), these thermodynamic arguments suggest that the neutral products formed are the covalently bound CoD rather than Co+D, whereas for reaction (6) the separated $Co+CD_3$ species appear to be formed.

A. $Co^+ + CD_4$

Previous experiments[49] show that atomic Co^+ ions react with CD_4 in endothermic processes and reactions (1)–(5) are all observed. The dominant reaction at all energies is formation of CoD^+ in reaction (1). Reactions (4) and (5) are observed to have similar threshold energies around 2 eV. Decomposition of the primary $CoCD_2^+$ and $CoCD_3^+$ products leads to the secondary products, CoC^+ and $CoCD^+$, at higher energies with small cross sections.

B. $Co_2^+ + CD_4$

Figure 1 shows results for reaction of the cobalt dimer cation with methane. Addition of the second cobalt atom increases the complexity of the reaction and reactions (1)–(6) and (8)–(11) are all observed. It seems likely that the failure to see CoC^+, reaction (7), is simply because its intensity is too small. The dominant process at all energies is hydride formation, Co_2D^+, reaction (1). At higher energies, Co_2D^+ can lose a cobalt atom to form CoD^+ in reaction (6). The lowest energy process observed is the formation of $Co_2CD_2^+$ in reaction (4), having an apparent threshold about 1.3 eV lower than that observed for the analogous reaction with Co^+. At higher energies, $Co_2CD_2^+$ can dissociate by cobalt atom loss to form $CoCD_2^+$ in reaction (9) by further dehydrogenation to form Co_2C^+ in reaction (2) (the dominant process), and by deuterium atom loss to yield Co_2CD^+ in reaction (3). The latter two channels show competition with one another. The $Co_2CD_3^+$ product dissociates to form $Co_2^+ + CD_3$, a process that can begin at 4.58 eV=D(D–CD_3), consistent with the energy where the $Co_2CD_3^+$ cross section begins to decline. The Co_2D^+ product could also begin to dissociate at this energy, but the observation that this does not occur indicates that the CD_3 product carries away most of the excess energy. Co_2CD^+ decomposes further by cobalt atom loss to form $CoCD^+$, a product that may also be formed by D atom loss from $CoCD_2^+$, by D_2 loss from $CoCD_3^+$, or by CoD loss from $Co_2CD_2^+$. CoD formation is suggested by thermodynamic arguments for formation of $CoCD^+$ at the threshold (see below). Given that the apparent thresholds of $Co_2CD_3^+$ and $CoCD_3^+$ product are similar, formation of $CoCD_3^+$ is likely to be accompanied by CoD, reaction (10), as verified by the thermochemical arguments discussed below.

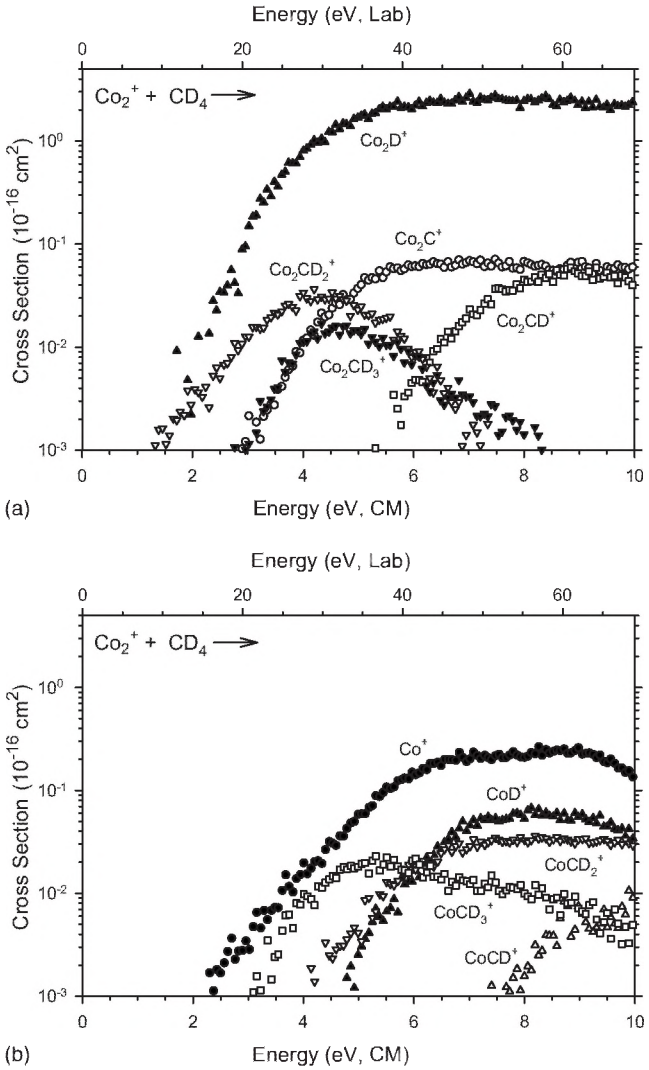

FIG. 1. Product cross sections for reaction of Co_2^+ with CD_4 as a function of collision energy in the CM (lower x-axis) and laboratory axis (upper x-axis). Parts (a) and (b) show cross sections for formation of $Co_2L^+ + (CD_4 - L)$ and $CoL^+ + Co + (CD_4 - L)$, respectively.

C. Co_3^+ and $Co_4^+ + CD_4$

Results for the trimer cobalt cation reacting with methane are shown in Fig. 2, where reactions (1)–(4) and (6)–(11) are all observed. The results are similar to those of the dimer, however, the $Co_3CD_3^+$ product of reaction (5) is absent in this system. The dominant process at all energies is hydride formation, Co_3D^+, reaction (1). Reaction (1) and the dehydrogenation reaction (4) are the lowest energy processes observed in reaction of the trimer. These two reactions compete with one another, as shown in Fig. 2(a). The $Co_3CD_2^+$ product can decompose by losing a D atom to form Co_3CD^+, a cobalt atom to form $Co_2CD_2^+$, and can also further dehydrogenate to form Co_3C^+. The latter dehydrogenation process is the dominant dissociation channel and appears to limit the magnitude of the $Co_2CD_2^+$ product cross section.

Co_3D^+ and Co_2^+ are the main products at higher energies. Co_2D^+ is formed by cobalt atom loss from Co_3D^+ in reaction (6). As for the dimer, the primary $Co_3CD_x^+$ (x=0–2) products decompose to yield $Co_2CD_x^+$ (x=0–2) products in reactions (7)–(9). Possible pathways for Co_2CD^+ and Co_2C^+ produc-

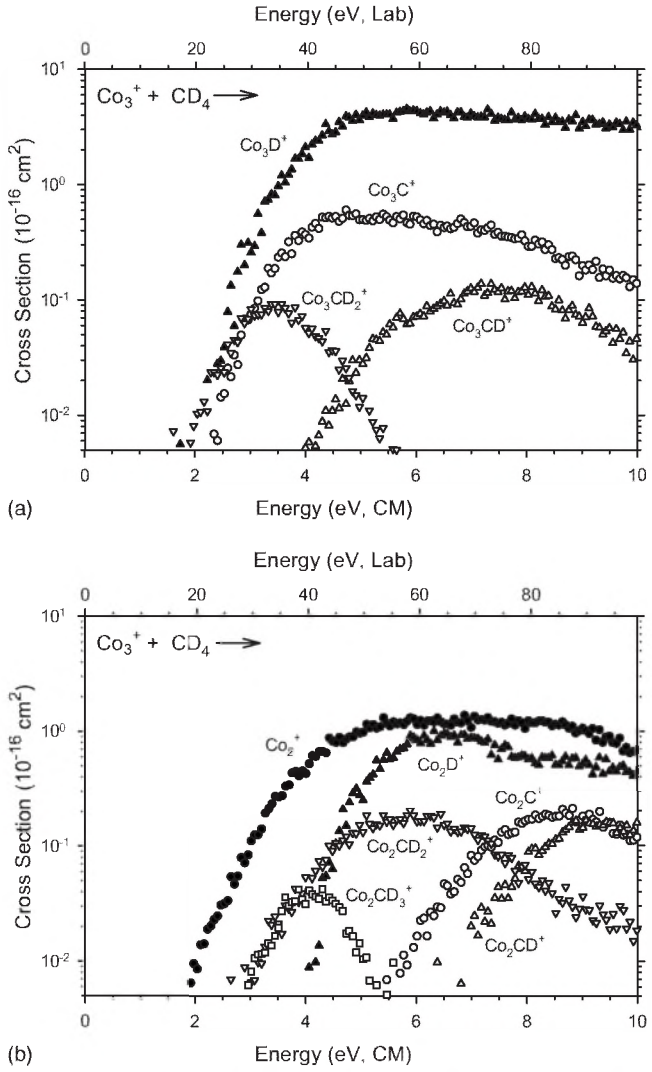

FIG. 2. Product cross sections for reaction of Co_3^+ with CD_4 as a function of collision energy in the CM (lower x-axis) and laboratory axis (upper x-axis). Parts (a) and (b) show cross sections for formation of $Co_3L^+ + (CD_4 - L)$ and $Co_2L^+ + Co + (CD_4 - L)$, respectively.

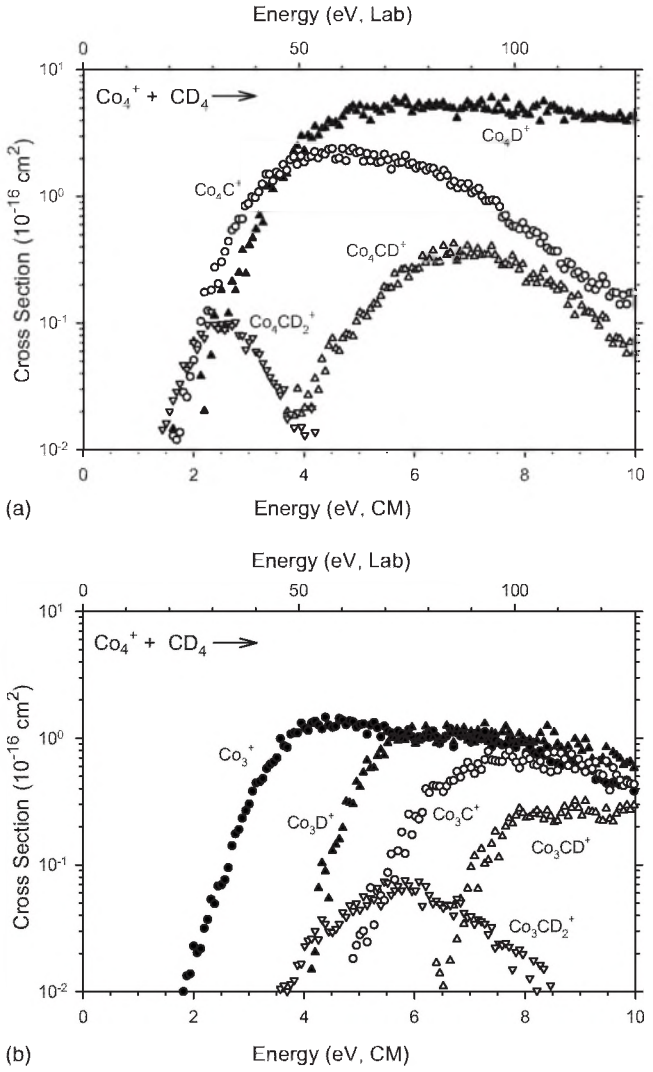

FIG. 3. Product cross sections for reaction of Co_4^+ with CD_4 as a function of collision energy in the CM (lower x-axis) and laboratory axis (upper x-axis). Parts (a) and (b) show cross sections for formation of $Co_4L^+ + (CD_4 - L)$ and $Co_3L^+ + Co + (CD_4 - L)$, respectively.

tion involve loss of a cobalt atom from the Co_3CD^+ and Co_3C^+ products, respectively, or loss of D and D_2 from $Co_2CD_2^+$, respectively. The Co_2CD^+ product can also be formed by loss of D_2 from $Co_2CD_3^+$ or CoD from $Co_3CD_2^+$. Because the $Co_2CD_2^+$ cross section falls as the Co_2CD^+ and Co_2C^+ cross sections increase, the losses of D and D_2 from $Co_2CD_2^+$ appear to be the dominant pathways. Co_2CD^+ is formed primarily by Co loss from Co_3CD^+ and Co_2C^+ is produced by cobalt atom loss from Co_3C^+. Formation of $Co_2CD_3^+$ is observed with a threshold that corresponds to production of a CoD neutral in reaction (10) (see below), and clearly cannot be formed by Co loss from $Co_3CD_3^+$, as no $Co_3CD_3^+$ is observed.

Figure 3 shows the reaction cross sections for the cobalt tetramer cation. Reactions (1)–(4), (6)–(9), and (11) are all observed, whereas formations of $Co_4CD_3^+$ and $Co_3CD_3^+$ products in reactions (5) and (10) are not found. The dehydrogenation reaction (4) is the lowest energy process for the tetramer. As for the trimer system, the Co_4C^+ product declines because of competition with Co_4D^+ formation, as no other product has a cross section with sufficient magnitude to account for the decline. This indicates that primary products, Co_4C^+ and Co_4D^+, compete with each other, which suggest that they share a common precursor, as discussed further below. The $Co_4CD_2^+$ product can decompose by losing a D atom to form Co_4CD^+ and a cobalt atom to form $Co_3CD_2^+$, and can also further dehydrogenate to form Co_4C^+ (the dominant process). Co_3CD^+ is also observed and is likely to be formed by Co loss from Co_4CD^+, with possible contributions from D atom loss from $Co_3CD_2^+$.

D. Co_n^+ (n=5–9)+CD_4

Figure 4 shows the cross sections for reaction of the cobalt heptamer cation with deuterated methane, which are representative of the n=5–9 clusters. Reactions (1)–(4), (6)–(8), and (11) are observed, although the cross sections for all reaction channels are relatively small for n=5–7. The primary dehydrogenation reaction (4) is particularly inefficient, which is partly because the subsequent dehydrogenation to form Co_nC^+ is a low energy and efficient process. Similar to

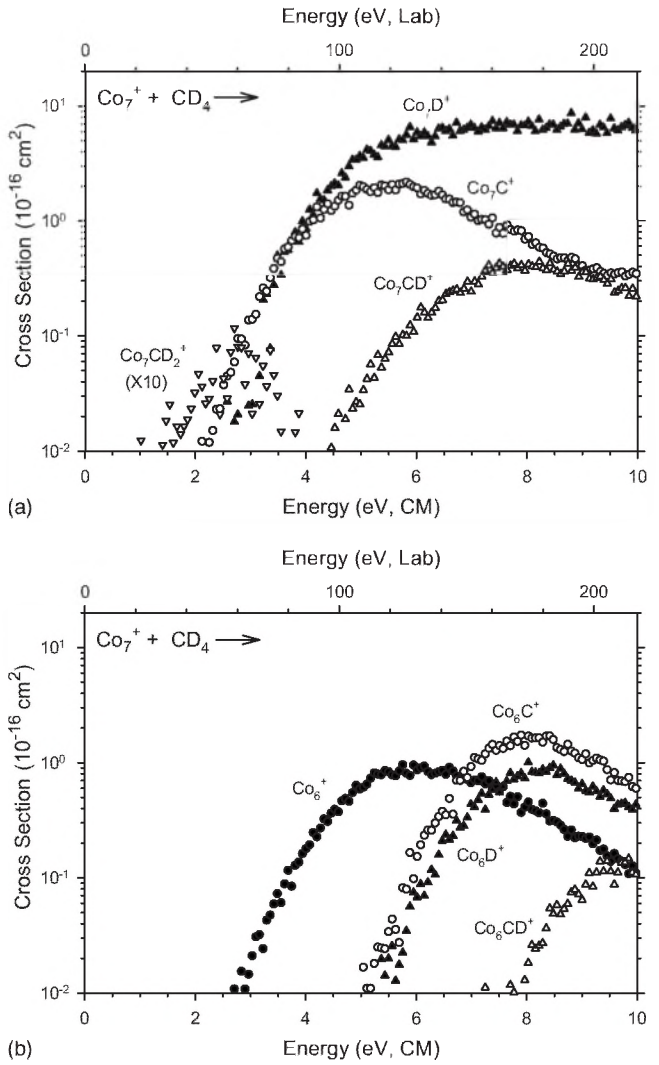

FIG. 4. Product cross sections for reaction of Co_7^+ with CD_4 as a function of collision energy in the CM (lower x-axis) and laboratory axis (upper x-axis). Parts (a) and (b) show cross sections for formation of $Co_7L^+ + (CD_4 - L)$ and $Co_6L^+ + Co + (CD_4 - L)$, respectively.

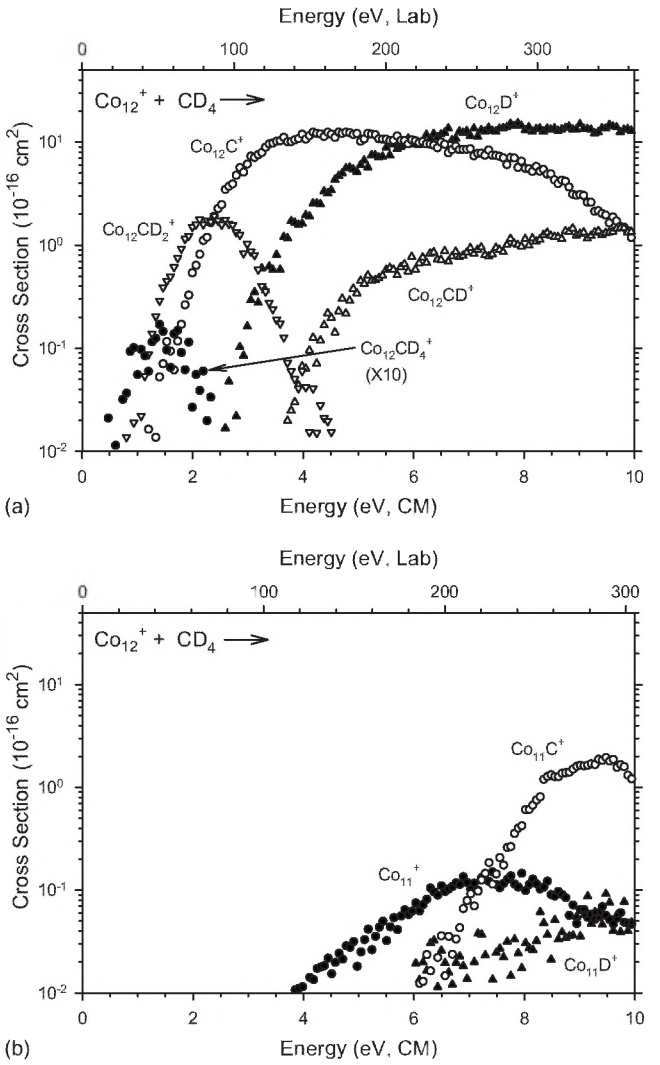

FIG. 5. Product cross sections for reaction of Co_{12}^+ with CD_4 as a function of collision energy in the CM (lower x-axis) and laboratory axis (upper x-axis). Parts (a) and (b) show cross sections for formation of $Co_{12}L^+ + (CD_4 - L)$ and $Co_{11}L^+ + Co + (CD_4 - L)$, respectively.

the reactions of smaller clusters, the Co_nC^+ cross sections decline largely at higher energies because of competition with Co_nD^+ formation, indicating that they must pass through a common intermediate. In contrast to smaller clusters, the secondary dehydrogenation product, $Co_{n-1}CD_2^+$, is absent for the $n=5-9$ clusters, which is an indirect confirmation that these species are formed by Co atom loss from the inefficiently formed $Co_nCD_2^+$ precursors.

E. Co_n^+ ($n=10-16$) + CD_4

Figure 5 shows results for reactions of the cobalt dodecamer cation with methane, which are representatives of larger clusters ($n=10-16$). Reactions (1)–(4), (7), and (11) are observed. Also, reaction (6) is observed for $n=10-12$ and reaction (8) for $n=10$ only. For $n=16$, the Co_{n-1}^+ product of reaction (11) is absent in this system. The feature that distinguishes these large clusters from the smaller systems is the observation of an adduct formed in process (12),

$$Co_n^+ + CD_4 \rightarrow Co_nCD_4^+. \quad (12)$$

We verified that this product was not the result of collisional stabilization by checking that the cross sections do not depend on CD_4 pressure. Thus, these species are observed because they have a lifetime in excess of the experimental time of flight between the collision cell and the detector, about 10^{-4} s. For smaller cluster sizes, the lifetimes of the adducts are too short for these products to be observed.

In contrast to small clusters, another difference in the results for these larger clusters is a gradual increase in the maximum magnitude in the cross section for the $Co_nCD_2^+$ dehydrogenation product as the cluster size increases, from 0.5 Å^2 for $n=10$ to about 4 Å^2 for $n=15$. The double dehydrogenation reactions to form Co_nC^+ are clearly facile in these systems, such that Co_nC^+ are the dominant products over a 2.5–4.5 eV range. $Co_{n-1}CD_2^+$ products are not observed for these larger clusters presumably because dehydrogenation of $Co_nCD_2^+$ is so efficient. Again the Co_nC^+ cross section declines as the Co_nD^+ rises, indicating competition between these two product ions. Formations of the secondary

$Co_{n-1}D^+$, $Co_{n-1}C^+$, and $Co_{n-1}CD^+$ products are similar to those for the smaller clusters, with magnitudes that track with those of the Co_nD^+, Co_nC^+, and Co_nCD^+ precursors.

F. Comparison to previous experimental results

These results differ dramatically from previous studies of Nakajima *et al.*[50] who studied the reactions at thermal energies of Co_n^+ ($n=2-22$)+CH_4 using a fast-flow reactor corresponding to high pressure multiple collision conditions. Under these experimental conditions, the only product observed was the adduct, whereas we observe no products at thermal energies under our single collision conditions. These differences in observation are clearly associated with the high pressure conditions that can stabilize a transient $Co_n^+(CH_4)$ adduct, where the methane molecule is probably physisorbed, given the energy thresholds observed here are for chemisorption in reaction (12). Interestingly, Nakajima *et al.*[50] do observe that the Co_6^+ cluster is particularly unreactive, in agreement with the trend in reactivity with cluster size observed here. They also find that cluster reactivity declines more or less monotonically from $n=10-22$, whereas we find a modest increase in reactivity over the range of $n=10-16$.

IV. THRESHOLD ANALYSIS AND THERMOCHEMISTRY

A. Data analysis

The energy dependence of cross sections for endothermic processes in the threshold region is modeled using Eq. (13),

$$\sigma(E) = \sigma_0 \sum g_i(E + E_i - E_0)^N/E, \tag{13}$$

where σ_0 is an energy independent scaling parameter, N is an adjustable parameter that describes the energy dependence, E is the relative kinetic energy, and E_0 is the threshold for reaction at 0 K. The summation is over the rovibrational states of the reactants having energies E_i and relative populations g_i, where $\Sigma g_i=1$. Vibrational frequencies associated with the bare metal cluster cation are calculated by using an elastic cluster model suggested by Shvartsburg *et al.*[51] A characteristic of this approach is the formal assignment of the vibrational models to one longitudinal and two transverse branches. The parameters used in this study are the Debye frequency for bulk cobalt, $\upsilon_D(\infty)=280$ cm^{-1}, the bulk maximum longitudinal frequency $\upsilon_{L,max}=301$ cm^{-1}, and the ratio of the longitudinal to the transverse phonon velocity $c_L/c_T=1.81$, which are estimated from the average values of bulk nickel[52,53] and bulk iron.[53–55] CD_4 vibrational frequencies are taken from the literature.[56] Before making comparison with the experimental data, the model cross section of Eq. (13) is convoluted with the kinetic energy distributions of the ion and neutral reactants.[47]

For metal clusters, it has been shown that lifetime effects become increasingly important as the size of the cluster increases[43] and need to be explicitly treated for the extraction of accurate thermochemical data from threshold experiments.[1,57–59] This is because metal clusters have many low frequency vibrational modes such that the lifetimes of some reaction intermediates can exceed the experimental time window (approximately 10^{-4} s in our apparatus) available for reaction. Thus, an important component of the modeling of these reactions is to include the effect of the lifetime of the reaction, as estimated using statistical Rice–Ramsperger–Kassel–Marcus (RRKM) theory.[60–62] This is achieved using an extension of Eq. (13), detailed elsewhere,[63] and requires molecular constants for the energized molecule (EM) and transition state (TS) leading to the product of interest. Three different TS models are employed: (a) A loose variational TS (LTS); (b) a tight fixed TS (TTS); and (c) a "standard" tight, fixed TS (STS). For the primary reactions leading to Co_nD^+ and $Co_nCD_2^+$ formation in reactions (1) and (4), the EMs are the transiently formed $Co_nCD_4^+$ complex, which we assume has a $D-Co_n^+-CD_3$ structure. For production of the secondary products, Co_nC^+ and Co_nCD^+ in reactions (2) and (3), we presume that the rate-limiting step is the second step, i.e., decomposition of the primary $Co_nCD_2^+$ product. Although it is possible that the rate-limiting step is the formation of the $Co_nCD_2^+$ species, this seems unlikely at the elevated energies needed to form these two products. The EM for the production of $Co_{n-1}D^+$ depends on whether reaction (6) generates Co+CD_3 or $CoCD_3$ neutral products. When the former products are formed in reaction (6), the EM is Co_nD^+, whereas the EM should be $DCo_nCD_3^+$ when $CoCD_3$ is formed. For the $Co_{n-1}CD_2^+$ products, observed only for the $n=2-4$ clusters, the EM is $Co_nCD_2^+$. For the $Co_{n-1}C^+$ products, the EM is assumed to be Co_nC^+, and for formation of $Co_{n-1}CD^+$, both $Co_nCD_2^+$ and $Co_{n-1}CD_2^+$ EMs are considered depending on whether CoD or Co+D products, respectively, are formed in reaction (8).

The vibrational frequencies for these various EMs are listed in Table S1 and estimated as follows. For all species, the $3n-6$ vibrations associated with the cluster are assumed to equal those of the bare cluster, as estimated using an elastic cluster model suggested by Shvartsburg *et al.*[51] For Co_nD^+, three additional frequencies are needed and are taken from our study of the reactions of Co_n^+ with D_2,[17] where the symmetric stretching (966 cm^{-1}), asymmetric stretching (885 cm^{-1}), and wagging (737 cm^{-1}) frequencies were estimated using a simple analysis. The ratios of the symmetric stretch to the asymmetric stretch (0.916) and to the wag (0.763) are used to estimate similar frequencies in several of the systems of interest here. For Co_nC^+ and Co_nCD^+, the additional frequencies are estimated from the average values of the vibrational frequencies for analogous carbide and carbyne iron and nickel clusters,[11,26] respectively. For $Co_nCD_2^+$, five of the frequencies (three vibrations of CD_2, the Co–C stretch, and an out-of-plane bend) are taken from measurements of $CoCD_2$.[64] The remaining four frequencies are scaled from the Co–C stretch and out-of-plane bend using the ratios from Co_nD^+. For the $D-Co_n^+-CD_3$ intermediate, the total number of vibrational frequencies is $3(n+5)-6$. Three of the additional 15 frequencies are associated with the Co_n^+-D motions and are taken from our previous work.[17] Six of these are associated with the internal motions of CD_3 and are taken as equal to those for free CD_3.[65] The stretching frequency for $Co_n^+-CD_3$ was taken from the average value of

the vibrational frequencies for analogous methylated iron and nickel clusters[11,26] and two additional modes were decreased from the stretching frequency using Co_nD^+ ratios. The three final frequencies were also set from the average value of the vibrational frequencies for analogous methylated iron and nickel clusters[11,26] and using Co_nD^+ ratios. In all cases, the cluster-ligand frequencies were assumed to remain constant for all cluster sizes. Although this is undoubtedly not precise, clusters differing by only one Co atom should have frequencies that do not differ appreciably. Further, in our analysis of the data, uncertainties are determined by scaling all the frequencies by ±50% to account for the uncertainties in the estimation of the frequencies.

The statistical treatment of lifetime effects also requires knowledge of the TSs for each reaction of interest. For most reactions, we assume a LTS located at the centrifugal barrier, a so-called phase space limit or orbiting TS, which is treated variationally as described in detail elsewhere.[63] For ion-molecule reactions having no barriers in excess of the reaction endothermicity, this is a reasonable assumption.[60] For LTSs, the frequencies needed are simply those of the products and are listed in Table S1. For all secondary reactions (where at least two neutral products are formed), product cross sections were analyzed by removing the energy needed to generate the precursor (EM) for the process under consideration. For instance, during the analysis of Co_nC^+ product cross section, the threshold energy measured for the $Co_nCD_2^+$ precursor is removed from the total energy available to the $Co_nCD_2^+$ EM as that energy is not available for D_2 loss from $Co_nCD_2^+$.

$Co_nCD_2^+$ product cross sections were analyzed using both a LTS and a TTS.[63] The TTS may be appropriate in this case because barriers in excess of the endothermicity have been observed in the dehydrogenation of methane by atomic Co^+ and by iron cluster cations.[49,11] In the atomic system, this barrier is associated with a four-centered TS in the exit channel,[66] and an analogous species is the assumed TTS for all clusters here. Although this TTS is believed to move to the entrance channel for larger clusters,[11] the molecular parameters assumed here should still be appropriate for estimating the kinetics associated with such a TTS. The three additional frequencies needed for the TTS are associated with Co_n^+–D motions and are taken by scaling the 966, 885, and 737 cm^{-1} frequencies by $2^{-0.5}$ to account for the decreased bond order in the TTS. For dissociation of the $DCo_nCD_3^+$ intermediate to $Co_nD^+ + CD_3$, a LTS is appropriate, however, the thresholds for this Co_nD^+ product channel are affected by the competition with the dehydrogenation reaction channel, which passes through the same intermediate. For some clusters, the competition is evident from the energy dependence of the cross sections, whereas for others, the effects of competition are less clear. We consider this possibility by analyzing the data in all cases using a statistical model for competition detailed elsewhere.[63]

Co_nC^+ product cross sections from reaction (2) were also analyzed using both LTS and TTS models because the mechanism for the first dehydrogenation of $Co_nCD_4^+$ to form $Co_nCD_2^+$ should be similar to the second dehydrogenation of $Co_nCD_2^+$ to form Co_nC^+. Most cluster-ligand frequencies were taken from the analogous four-centered TS for dehydrogenation of $D–Co_n^+–CD_3$ to form $Co_nCD_2^+$, Table S1. For reactions in which a Co atom or a CoD neutral is lost to form $Co_{n-1}CD_x^+$ products, there are two reasonable choices for the type of TS: Either a LTS or a somewhat tighter TS, which has been dubbed a STS,[67] similar to that assumed for dissociation of bare Co clusters.[41] The former type of TS was assumed in our previous work on the reactions of Co cluster cations with O_2,[25] which yielded reasonable cluster oxide bond energies. Both assumptions are explored in this work.

Rotational constants for the various EMs and TSs were assumed to equal those of the bare clusters for all species except those involving the cobalt dimer and trimer. Rotational constants for $Co_2CD_x^+$ and $Co_3CD_x^+$ were estimated explicitly, as illustrated here for the examples of $Co_2CD_3^+$ and $DCo_2CD_3^+$. We assume that both of these have C_{3V} symmetry with bond lengths of 2.2 Å for Co–Co, 2.1 Å for Co–C, 1.1 Å for C–D, and 1.6 Å for Co–D.[66] These yield rotational constants of $A \sim 2.60$ cm^{-1} and $B = C \sim 0.05$ cm^{-1} for both species. For the trimer species, the metal framework is assumed to have an equilateral triangular structure with Co–Co bond lengths of 2.2 Å. Modeling of the cross section data is not particularly sensitive to the detailed rotational or vibrational constants chosen.

B. Primary and secondary reactions

In cluster studies, identical product ions are observed in both primary and secondary reactions. Thus, a species such as Co_nL^+ is formed as a primary product of Co_n^+ in reaction (14), and a secondary product of Co_{n+1}^+ in reactions (15) or (16), where $(CD_4–L)$ is the fragment remaining after removing L from CD_4.

$$Co_n^+ + CD_4 \rightarrow Co_nL^+ + (CD_4 - L), \quad (14)$$

$$Co_{n+1}^+ + CD_4 \rightarrow Co_nL^+ + Co + (CD_4 - L), \quad (15)$$

$$Co_{n+1}^+ + CD_4 \rightarrow Co_nL^+ + Co(CD_4 - L). \quad (16)$$

Hence, we generally have two independent means of determining the thermochemistry of each of the Co_nL^+ products. It is possible that thresholds obtained for the secondary reactions (15) could be higher than thermodynamic values if the total energy available in reaction (15) is not efficiently retained by $Co_{n+1}L^+$ precursors. However, if we assume that the energy is divided among the primary products statistically, we can expect that the $Co_{n+1}L^+$ product will retain much more energy than the $CD_4–L$ product, which has many fewer degrees of freedom. Similar considerations hold for alternate mechanistic pathways for the secondary reactions. Clearly, this assumption could degrade for the smallest clusters, and we explicitly consider this question below.

Bond energies of clusters can be obtained from the thresholds for reactions (14)–(16) using Eqs. (17)–(19),

$$D(Co_n^+ - L) = D(CD_4 - L) - E_0(14), \quad (17)$$

$$D(Co_n^+ - L) = D(CD_4 - L) + D(Co_n^+ - Co) - E_0(15), \quad (18)$$

TABLE I. Co_n^+–D bond energies (eV) obtained from the literature and analyses of reactions (1) and (6).

n	Co_n^+–D [a]	Co_n^+–D (1)[b]	Co_n^+–D (6)[c]	Co_n^+–D (Avg)[d]
1	2.03 ± 0.06 [e]		1.87 ± 0.17	2.01 ± 0.06
2	2.35 ± 0.09	2.28 ± 0.08	2.20 ± 0.20	2.30 ± 0.06
3	1.99 ± 0.11	1.96 ± 0.09	2.25 ± 0.18	2.01 ± 0.06
4	2.25 ± 0.16	2.14 ± 0.10	2.35 ± 0.23	2.19 ± 0.08
5	2.15 ± 0.23	1.98 ± 0.09	2.03 ± 0.23	2.01 ± 0.08
6	2.27 ± 0.29	1.79 ± 0.12	1.99 ± 0.23	1.88 ± 0.10
7	2.17 ± 0.29	1.81 ± 0.13	2.25 ± 0.28	1.93 ± 0.11
8	2.19 ± 0.31	1.90 ± 0.12	1.81 ± 0.23	1.91 ± 0.10
9	2.36 ± 0.33	2.07 ± 0.12		2.10 ± 0.11
10	2.47 ± 0.35	2.22 ± 0.10		2.24 ± 0.10
11	2.47 ± 0.36	2.34 ± 0.14		2.36 ± 0.13
12	2.53 ± 0.37	2.32 ± 0.14		2.35 ± 0.13
13	2.65 ± 0.35	2.39 ± 0.14		2.43 ± 0.13
14	2.67 ± 0.35	2.38 ± 0.14		2.42 ± 0.13
15	2.67 ± 0.35	2.55 ± 0.15		2.57 ± 0.14
16	2.69 ± 0.37	2.54 ± 0.14		2.56 ± 0.13

[a]From reactions of $Co_n^+ + D_2$, Ref. 17.
[b]Values obtained from analyses of reactions (1) assuming LTS and explicit competition with reactions (4).
[c]Average bond energies obtained from analyses of $Co_{n-1}D^+$ cross sections assigned to reactions (6) assuming LTS and STS models.
[d]Weighted average of all available values.
[e]Reference 85.

$$D(Co_n^+ - L) = D(CD_4 - L) + D(Co_n^+ - Co) - E_0(16) - D[Co - (CD_4 - L)], \quad (19)$$

where $D(CD_4–L)$ is the energy required to remove L from CD_4. In Eqs. (18) and (19), the dissociation energies for the bare Co_n^+ clusters are taken from previous studies in our laboratory.[41] In the present work, neutral $Co(CD_4–L)$ species considered include CoD and $CoCD_3$, which have $D[Co–(CD_4–L)]$ bond energies of 1.90 ± 0.05 and 1.89 ± 0.08 eV, respectively.[68]

C. Thermochemical results

1. Co_n^+–D

Bond energies for Co_nD^+ have previously been measured by threshold analyses of the endothermic reactions of Co_n^+ clusters with D_2,[17] and are listed in Table I. In the present study, this thermochemistry can be obtained from analyses of the cross sections for reactions (1) and (6). Needed thermodynamic information includes $D(CD_3–D) = 4.58 \pm 0.01$ eV.[69,70] Reactions (1) were analyzed using a LTS coupled with explicit consideration of the competition[71] with the low energy dehydrogenation channel, reaction (4), assumed to have a TTS. Bond energies obtained from these analyses are listed in Table I and shown in Fig. 11S.[48] These values are in good agreement with the previous data,[17] with a mean absolute deviation (MAD) of 0.21 ± 0.12 eV for $n = 2–16$. The competition threshold analysis has no additional optimizing parameters (other than the threshold energies for each channel) to adjust compared to the normal threshold analysis (including lifetime effects).[71] The competition between channels is determined by the ratio of the unimolecular rate constants for each process, as calculated using RRKM theory. Thresholds for both reactions (1) and (4) are simultaneously obtained in this procedure. Bond energies obtained from thresholds for reactions (1) that do not include competition are in much worse agreement with the previous thermochemistry for $D(Co_n^+–D)$.

Co_n^+–D bond energies obtained from analyses of the secondary reactions (6) are also listed in Table I (see also Fig. 11S).[48] The data for reactions (6) were analyzed assuming both a LTS and a STS. When the neutral products are assumed to be $Co+CD_3$, the average bond energies for $n = 1–8$ obtained using these two models are in good agreement with the previously published values[17] (MAD = 0.19 ± 0.10 eV). Hence, our assumption that energy is efficiently retained by the primary product (Co_nD^+) appears to be reasonable, even for these smaller clusters. For clusters larger than $n=8$, the secondary $Co_{n-1}D^+$ product cross sections are too small to be reliably analyzed. Clearly, if the neutral products of reactions (6) are assumed to be $CoCD_3$, the Co_n^+–D bond energies derived would decrease by $D(Co–CD_3) = 1.89 \pm 0.08$ eV (Ref. 68) according to Eq. (19), making them much lower than previous results.

2. Co_n^+–CD_3

Cobalt cluster methyl cations are observed only in the reactions of the dimer and trimer cations. For dimer reactions, the thresholds for $Co_2CD_3^+$ and $CoCD_3^+$ are 2.57 ± 0.14 and 3.36 ± 0.15 eV, respectively (Table S2).[48] The bond energy $D(Co_2^+–CD_3)$ of 2.01 ± 0.14 eV can be obtained according to Eq. (17). If we assume that the secondary methyl product is formed along with CoD in reaction (10), Eq. (19) can be used to convert the latter threshold to a $Co^+–CD_3$ bond energy of 2.09 ± 0.16 eV. This value for $CoCD_3^+$ agrees well with a bond energy previously determined for $CoCH_3^+$, 2.10 ± 0.04 eV.[49,72] The other possibility for the secondary reaction is concomitant formation of Co+D, which gives a bond energy of 3.99 ± 0.15 eV for $Co^+–CD_3$. Clearly, $CoCD_3^+$ is formed in process (10) along with CoD as a neutral product in the reaction of the dimer cobalt cation.

For the trimer cobalt cation, only a secondary methyl product is observed in reaction (10). The bond energy $D(Co_2^+–CD_3) = 2.22 \pm 0.19$ eV can be obtained from the threshold (2.55 ± 0.13 eV) using Eq. (19). This value is within experimental uncertainty of that obtained from the dimer cation reaction. Thus, formation of $Co_2CD_3^+$ is accompanied by loss of neutral CoD. We take the weighted average value of 2.08 ± 0.11 eV as our best determination of the $Co_2^+–CD_3$ bond energy. Larger clusters do not produce $Co_nCD_3^+$ or $Co_{n-1}CD_3^+$ with any efficiency, apparently because they have more facile decomposition pathways than loss of D or CoD from the transient $Co_nCD_4^+$ intermediate.

3. Co_n^+–CD_2

Bond energies for $Co_n^+–CD_2$ can be obtained from analyses of the thresholds for reactions (4) and (9) using Eqs. (17) and (18), respectively. The required thermochemistry is $D(CD_2–D_2) = 4.82 \pm 0.03$ eV.[69] The data for reactions (4) were analyzed assuming both a LTS and a TTS. Competition with reaction (1) is also explicitly considered but this does

TABLE II. Co_n^+–CD_2 bond energies (eV) obtained from analyses of reactions (4) and (9).

n	Co_n^+–CD_2 (4) (LTS)	Co_n^+–CD_2 (4) (TTS)	Co_n^+–CD_2 (9)[a]
1		3.32 ± 0.05 [b]	3.35 ± 0.18
2	3.05 ± 0.13	3.08 ± 0.11	3.77 ± 0.18
3	2.93 ± 0.09	3.07 ± 0.09	3.77 ± 0.18
4	3.26 ± 0.09	3.46 ± 0.09	
5	3.35 ± 0.10	3.58 ± 0.10	
6	~3.2 [c]	~3.5 [c]	
7	~3.1 [c]	~3.5 [c]	
8	3.00 ± 0.09	3.44 ± 0.10	
9	3.08 ± 0.09	3.51 ± 0.09	
10	3.27 ± 0.09	3.67 ± 0.09	
11	3.33 ± 0.09	3.75 ± 0.09	
12	3.40 ± 0.09	3.77 ± 0.09	
13	3.50 ± 0.09	3.87 ± 0.08	
14	3.43 ± 0.08	3.83 ± 0.09	
15	3.54 ± 0.09	3.94 ± 0.09	
16	3.45 ± 0.08	3.88 ± 0.09	

[a]Average bond energy obtained from LTS and STS models.
[b]Reference 49.
[c]Because of the small size of these cross sections, only rough estimates of the threshold could be obtained.

not alter the thresholds obtained for reaction (4). Those bond energies are given in Table II. We find that the values derived assuming a LTS are on average 0.41 ± 0.03 eV lower than those for a TTS for $n=7-16$. We also analyzed the secondary reactions (9) corresponding to loss of a Co atom from the $Co_nCD_2^+$ primary products, which are only observed for reactions of $n=2-4$ cations. The TSs are treated with both LTS and STS models, with Table II reporting the average bond energy derived from these analyses.

For reaction of Co_2^+ to form $CoCD_2^+$ in process (9), the thresholds obtained using LTS and STS models correspond to Co^+–CD_2 bond energies of 3.19 ± 0.18 and 3.51 ± 0.17 eV, respectively. Either value is within experimental uncertainty of the literature bond energy, 3.32 ± 0.05 eV,[70,73] and the average of the LTS and STS model results, 3.35 ± 0.18 eV, is listed in Table II. Notably, the literature bond energy for Co^+–CD_2 was not measured in reaction (4) of the monomer cation, $Co^+ + CD_4 \rightarrow CoCD_2^+ + D_2$, as this gives a bond energy of 0.72 ± 0.24 eV lower than the thermodynamic value because the threshold for this reaction corresponds to a barrier attributed to a four-center TS in the exit channel.[49] A more precise measure of the barrier height is 0.35 ± 0.08 eV as measured by examining the reverse process, $CoCH_2^+ + D_2 \rightarrow Co^+ + CH_2D_2$.[49] For reaction of Co_3^+ to form $Co_2CD_2^+$, the threshold obtained from analysis of reaction (9) using a LTS corresponds to a bond energy of 3.64 ± 0.18 eV, well above the value derived from reaction (4), 3.08 ± 0.11 eV, Table II. The result for reaction (9) is not particularly sensitive to the type of TS as the bond energy obtained using a STS is 3.91 ± 0.18 eV. In analogy with the dimer reaction, the discrepancy between the results for the primary and secondary reactions is sensibly attributed to a barrier along the reaction path for dehydrogenation in reaction (4). This indicates that the use of the TTS model for reaction (4) is appropriate. Using the average LTS and STS bond energy derived from reaction (9), 3.77 ± 0.18 eV, the barrier for reaction of the trimer cation is measured to be about 0.69 ± 0.21 eV, comparable to the value for the monomer. For reaction of Co_4^+, the average $Co_3CD_2^+$ bond energy obtained from analysis of reaction (9) using LTS and STS models, 3.77 ± 0.18 eV, is again well above those obtained for reaction (4) of Co_3^+ using the TTS assumption in the analysis, Table II. These results indicate that there is again a barrier for reaction (4) of the tetramer cation of about 0.70 ± 0.20 eV.

For larger clusters, $n=4-16$, the secondary reactions (9) are not observed, as was also found for reactions of nickel cluster cations with methane.[26] In contrast, primary and secondary paths were observed for all cluster sizes in the dehydrogenation reactions of iron cluster cations with methane.[11] For Fe_n^+ ($n=5-15$), the primary dehydrogenation reactions exhibited barriers, assigned to the entrance channel. The barrier height averaged 0.7 ± 0.3 eV, essentially the same value obtained here for Co_n^+ ($n=1-3$). In analogy with these results, the primary dehydrogenation reactions for larger cobalt clusters seem likely to have barriers in the entrance channel as well. Thus, bond energies $D(Co_n^+–CD_2)$ ($n=4-16$) obtained here for reactions (4) using a TTS model are conservatively thought to be lower limits to the true thermochemistry. We estimate that the true bond energies can be approximated by adding 0.7 ± 0.2 eV to these values.

4. Co_n^+–C and Co_n^+–CD

Bond energies for Co_n^+–C can be obtained from analyses of reactions (2) and (7). Here, the required thermochemistry is $D(CD_4\text{-}L)=D(CD_2\text{-}D_2)+D(C\text{-}D_2)=8.20 \pm 0.04$ eV.[69] For reaction (2), the precursors are the primary $Co_nCD_2^+$ products, whereas for reaction (7), they are assumed to be the Co_nC^+ products. The average bond energies obtained from reactions (7) using the average of LTS and STS models agree well with the results obtained from analyses of reactions (2) using a TTS model (MAD = 0.19 ± 0.12 eV), well within experimental uncertainties. These bond energies are listed in Table III and shown in Fig. 13S.[48] Thresholds from the primary reactions (2) are more precise and therefore taken to be our best determination of bond energies for several reasons. (a) The mass overlap adjustments for the Co_nC^+ cross sections are less ambiguous compared to cross sections for $Co_{n-1}C^+$ formed in reaction (7). (b) Thresholds for reactions (7) occur at high energies, such that there are fewer data points for modeling given our energy range of 10 eV (CM). (c) Thresholds for reactions (7) could be shifted to higher energies by competition with the more efficient low energy processes or shifted as a consequence of the multiple neutral products carrying away excess energy.

Bond energies for Co_n^+–CD can be obtained from analyses of reactions (3) and (8). The required thermochemistry is $D(CD_4\text{-}L)=D(CD_2\text{-}D_2)+D(CD\text{-}D)=9.25 \pm 0.04$ eV.[69] For reactions (3) and (8), the precursors are the primary $Co_nCD_2^+$ products. Therefore, cross sections are analyzed for thresholds using LTS models associated with D atom loss for reactions (3) and CoD loss for reactions (8). The results are given in Table IV and also shown in Fig. 14S of the supple-

TABLE III. Co_n^+–C bond energies (eV) obtained from analyses of reactions (2) and (7).

n	Co_n^+–C (2) (TTS)	Co_n^+–C (7)[a]
1	3.60 ± 0.30 [b]	
2	4.94 ± 0.11	4.73 ± 0.18
3	5.46 ± 0.10	5.14 ± 0.19
4	5.93 ± 0.11	5.81 ± 0.20
5	5.93 ± 0.10	5.88 ± 0.24
6	5.33 ± 0.14	5.54 ± 0.23
7	5.48 ± 0.14	5.48 ± 0.27
8	5.59 ± 0.16	5.39 ± 0.26
9	5.75 ± 0.16	5.51 ± 0.26
10	6.02 ± 0.17	5.90 ± 0.31
11	6.14 ± 0.18	6.01 ± 0.36
12	6.17 ± 0.18	6.31 ± 0.39
13	6.29 ± 0.19	5.85 ± 0.41
14	6.25 ± 0.17	6.56 ± 0.44
15	6.40 ± 0.21	6.28 ± 0.44
16	6.31 ± 0.21	

[a]Average bond energies obtained from LTS and STS models.
[b]Reference 49.

mentary material.[48] Bond energies obtained from analyses of reactions (8) are in good agreement with the bond energies obtained from reaction (3), except for $n=4$. Overall, the two sets of data have a MAD of 0.21 ± 0.12 eV for $n=1-7$. Thresholds from the primary reactions (3) are more reliable and precise and therefore taken to be our best determination of bond energies. The reasons for the higher reliability are the same as those listed above for the Co_n^+–C bond energies.

5. Co^+–CD_4

For clusters with $n \geq 10$, we observe the $Co_nCD_4^+$ adduct. Unfortunately, because of their small magnitudes, the quality of these cross sections is not sufficient to analyze using Eq. (13). A qualitative analysis of these processes was obtained by analyzing the sum of the $Co_nCD_4^+$, $Co_nCD_2^+$, and Co_nC^+ product cross sections using a TTS. In all cases, the measured thresholds are the same as those listed in Tables S10–S16 for the $Co_nCD_2^+$ product ion within 0.1 eV, consistent with the hypothesis that both product ions are limited by the same TS.

TABLE IV. Co_n^+–CD bond energies (eV) obtained from analyses of reactions (3) and (8).

n	Co_n^+–CD (3) (LTS)	Co_n^+–CD (8)[a]
1	4.37 ± 0.38 [b]	4.06 ± 0.23
2	3.98 ± 0.21	4.20 ± 0.22
3	5.16 ± 0.18	4.96 ± 0.22
4	5.54 ± 0.17	5.09 ± 0.23
5	5.20 ± 0.16	5.00 ± 0.28
6	4.80 ± 0.18	4.68 ± 0.28
7	4.75 ± 0.21	4.68 ± 0.32
8	5.33 ± 0.25	
9	5.70 ± 0.23	
10	5.87 ± 0.21	
11	5.70 ± 0.21	
12	5.86 ± 0.23	
13	5.89 ± 0.25	
14	6.05 ± 0.25	
15	5.94 ± 0.23	
16	6.13 ± 0.24	

[a]Average bond energies obtained from LTS and STS models.
[b]Reference 49.

Observation of the $Co_nCD_4^+$ product is expected only if its lifetime exceeds or is on the order of the detection time window of our instrument, 10^{-4} s. The reason that we do not observe any $Co_nCD_4^+$ products for many smaller clusters, $n=1-9$, is probably because these species dissociate more rapidly than this time window, even at low kinetic energies. The $Co_nCD_4^+$ product ions can possibly have one of two forms: (1) A physisorbed state, $Co_nCD_4^+$, a weakly bound adduct held together by ion-induced dipole attractions; or (2) a dissociative chemisorbed state, D–Co_n^+–CD_3, a strongly bound species where both ligands are chemically bonded to the cluster. A weakly bound physisorbed species should exhibit no activation barrier for its formation (because of the long-range ion-induced dipole attractive forces) and should have a fairly short lifetime because loss of an intact methane molecule should be facile. Such species are unlikely to survive our instrumental flight time, unless they are collisionally stabilized by multiple collisions with CD_4. Our pressure-dependent studies verify that the $Co_nCD_4^+$ products observed are not the result of collision stabilization. Thus, the adduct cross sections are likely to correspond to chemisorbed structures, which means that the threshold corresponds to the activation energy for chemisorption, probably C–D bond activation in the present cases. Assignment of these species to chemisorbed methane would help explain why such species are observed, as their lifetime must exceed the $\sim 10^{-4}$ s flight time of the ions in our instrument. Desorption of methane to return to reactants requires coupling of two or more fragments, which may now be remote from each other on the cluster surface, such that the lifetime of the $Co_nCD_4^+$ species could increase dramatically. This is especially true for the largest clusters, where the energy needed to eliminate methane has been dissipated throughout the cluster. Further evidence for a chemisorption structure is the observation that the cross sections for $Co_nCD_4^+$ decline as the $Co_nCD_2^+$ products of reactions (4) appear. As the latter clearly require activation of two CD bonds in methane, a D–Co_n–CD_3^+ species is an obvious precursor for reactions (1), (4), and (5).

V. DISCUSSION

A. Bond energies

Our recommended bond energies between cobalt cluster cations and the D and CD_x ($x=0-3$) ligands are shown in Fig. 6. The Co_n^+–D values are taken from our previous $Co_n^+ + D_2$ study.[17] Present Co_n^+–D results from the CD_4 reaction system substantiate the values from earlier work. The previous Co_n^+–D values are considered our best values because the analyses of the D_2 reaction cross sections involve no competition with other product channels and therefore are less complicated than those for the CD_4 reaction system. The bond energies of Co_n^+–C are obtained from analyses of reactions (2) with a TTS in all cases, Table III; whereas those for Co_n^+–CD are LTS results for reactions (3), Table IV, except

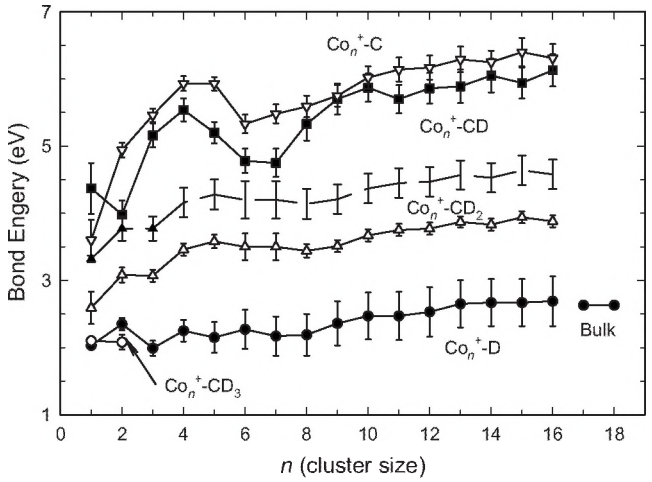

FIG. 6. Comparison of bond energies for Co_n^+–D (solid circles, taken from Ref. 17). Co_n^+-CD_3 (open circles, Ref. 72 and this work). Co_n^+–CD_2 (open triangles show values from reaction (4) taken from Ref. 72 and this work. Table II; solid triangles show values from reaction (9) and Ref. 72; the dashed line shows our best estimate of the values for larger clusters, see text). Co_n^+–CD (solid squares, this work, Table IV), and Co_n^+–C (open inverted triangles, this work, Table III). The bulk-phase value for cobalt surfaces binding D (average of Refs. 18–20) is also shown.

for $n=1$ values, which are taken from our previous work on reaction of $Co^+ + CH_4$.[49] As noted earlier, the Co_n^+–C and Co_n^+–CD values from reactions (2) and (3) are substantiated reasonably well by results for the secondary reactions (7) and (8), respectively. The Co_n^+–CD_2 values obtained from reactions (4) using a TTS model, Table II, are shown along with the $CoCD_2^+$ value taken from the literature,[49] and $Co_2CD_2^+$ and $Co_3CD_2^+$ values, which are obtained from reaction (9) using the average thresholds obtained from LTS and STS assumptions. As noted above, the values from reactions (4) are believed to be the lower limits to the true thermochemistry, as verified for the cases of $n=1-3$. Our best estimates of the true Co_n^+–CD_2 bond energies are shown as a dashed line in Fig. 6.

The trend of bond energies of these cluster-ligand complexes can be understood by considering the maximum number of bonds that the ligands can make with the cluster. D (^2S) and CD_3 ($^2A_1$) can make only a single covalent bond with the cluster, whereas CD_2 ($^3B_2$) can make two covalent bonds. CD can make three covalent bonds, but this requires promotion to the $\tilde{a}\ ^4\Sigma^-$ state, which is 0.72 eV above the $X\ ^2\Pi_r$ ground state.[74] The carbon atom has a ground state electronic configuration of $(2s)^2(2p)^2$ such that it can form two covalent bonds and accept electron density into the empty $2p$ orbital to form a third, dative bond. It can be seen that the Co_n^+–D and Co_n^+–CD_3 ($n=1$ and 2) bond energies are comparable. The estimated Co_n^+–CD_2 bond energies lie an average of 1.93 ± 0.08 eV higher in energy than the Co_n^+–D values for $n \geq 3$ ($>1.23 \pm 0.08$ eV if the lower limits for Co_n^+–CD_2 are used). Co_n^+–CD and Co_n^+–C bond energies are higher than the Co_n^+–D values by 3.17 ± 0.28 and 3.54 ± 0.19 eV, respectively, for $n \geq 3$. The Co_n^+–CD_2, Co_n^+–CD, and Co_n^+–C bond energies are average of 1.8 ± 0.1 ($>1.5 \pm 0.1$), 2.3 ± 0.1, and 2.5 ± 0.1 times stronger, respectively, than the Co_n^+–D bond energies for $n \geq 3$. These ratios agree with those observed in literature,[72] where double bonds should be about 1.7 times stronger than single bonds (the ratio of H_3C-CH_3 to $H_2C=CH_2$ and M^+-CH_3 to $M^+=CH_2$ bond energies) and triple bonds should be about 2.5 times stronger than single bonds (the ratios of H_3C-CH_3 to $HC\equiv CH$ and M^+-CH_3 to $M^+\equiv CH$ bond energies). These observations are qualitatively consistent with formation of single (D and CD_3) versus double (CD_2) versus triple (CD and C) bonds, as anticipated from the bonding character of the ligands.

In our previous work,[17] the Co_n^+–D bond energies were found to parallel Co_n^+–Co bond energies for many cluster sizes. The patterns in $D(Co_n^+-D)$ as a function of cluster size were used to qualitatively probe the cluster geometry and electronic configuration. Compared to the metal-metal (Co_n^+–Co) bonds, the cobalt-deuteride bonds are generally weaker, except for $n=2$. For most cluster sizes ($n=1$, 4, 6, 8–10, and 13), the average enhancement of 0.66 ± 0.1 eV can be attributed to metal-metal bonds enhanced by both $4s$-$4s$ and $3d$-$3d$ interactions. However, the enhancement is nonmonotonic at Co_5^+–Co, Co_7^+–Co, Co_{12}^+–Co, and Co_{14}^+–Co, with metal-metal bond energies being stronger by 1.13 ± 0.1 eV than the respective Co_n^+–D bond energies. This is believed to be because the Co_6^+, Co_8^+, Co_{13}^+, and Co_{15}^+ clusters have particularly stable geometries, such that substitution of a cobalt atom by D breaks the symmetry of the cluster, thereby affecting its stability. This stability is a likely reason that the Co_6^+ cluster has a particularly low reactivity. The other stable clusters may be more reactive because they are larger, thereby allowing a longer lifetime for interaction of the cluster with methane.

Information about the bonding of CD_2 to cobalt clusters is speculative and structures of these clusters are not known. As noted above, the bond energies of CD_2 to Co_n^+ clusters indicate that two bonds are formed. Presumably, CD_2 could bind terminally to the cluster by forming a σ and a π bond with a single metal atom or could bridge across two metal centers by forming two σ bonds. Co^+ ($^3F, 3d^8$) must bind to CD_2 terminally and has a bond energy weakened by the need to spin decouple two $3d$ electrons from the other nonbonding $3d$ electrons. This promotion energy lowers the Co^+–CD_2 bond energy (3.32 ± 0.05 eV) from an intrinsic metal-carbon double bond energy of about 4.3 ± 0.1 eV.[72,75] Notably, this intrinsic metal-carbon double bond energy closely matches the estimated Co_n^+–CD_2 bond energies for larger clusters ($n \geq 10$), 4.5 ± 0.2 eV. In addition, the estimated Co_n^+–CD_2 bonds are stronger than Co_n^+–D bonds by 1.93 ± 0.08 eV for $n=3-16$, which is comparable to the intrinsic metal-carbon π bond strength of 1.8 eV.[72] These observations are therefore consistent with the estimate that there are barriers of about 0.7 ± 0.2 eV to the formation of Co_n^+–CD_2 in reactions (4), as discussed further below.

Bonds between CD and C ligands and the Co^+ monomer (Co^+–CD and Co^+–C) and dimer (Co_2^+–CD) are weaker than those for larger clusters. The bond energies of Co_n^+–CD_2 and Co_2^+–CD are quite similar, with magnitudes that suggest that the cobalt dimer cation can form two covalent bonds, but that the promotion energy to form a third covalent bond is prohibitive. These ligands can potentially bind to clusters in different ways: Terminal, twofold bridging, and threefold

bridging. An obvious implication of the strength of the CD and C bonds relative to CD_2 bonds for the trimer and larger clusters is that binding to three atoms in a threefold site may provide the strongest bond energies, consistent with the known structure of alkylidynes bound to many surfaces.[76] Theoretical studies of these small molecules would be of interest in further understanding these trends. For $n \geq 3$, the binding energies of CD and C to cobalt cluster cations are large and do not vary significantly after $n \geq 9$. The Co_n^+–CD bond energies increase somewhat as the cluster size increases, such that the average bond dissociation energies are 5.21 ± 0.36 eV for $n=3-8$ and 5.92 ± 0.14 eV for $n=9-16$. The Co_n^+–C bond energies are stronger than $D(Co_n^+-CD)$ by an average of 0.43 ± 0.25 eV for $n=3-8$ and by 0.31 ± 0.13 eV for $n=9-16$, where they parallel one another. This difference may be explained by the following argument. Carbon ($^3P, s^2p^2$) atom can potentially form two covalent bonds with metals and possibly augment these bonds by accepting a pair of electrons into the empty $2p$ orbital on carbon. In contrast, CD ($^4\Sigma^-$) could form a triple bond although this requires excitation from the $^2\Pi$ ground state (0.72 eV),[74] thereby lowering the final bond energy to cobalt clusters. Overall, these observations suggest that cobalt clusters have substantial flexibility in making the strongest possible bond to molecular fragments.

B. Bond energies compared to analogous iron and nickel clusters

It is useful to compare the binding of D and CD_x species to cobalt cluster cations with that to iron and nickel cluster cations.[11,26] For small clusters, the bond energies for D and CD_x to Co_n^+, Fe_n^+, and Ni_n^+ vary considerably with cluster size, indicating changes in the electronic structure of the metal clusters.[11,26]

For the dimers, D, CD_3, CD_2, CD, and C bind to Co_2^+ more strongly than to Fe_2^+ by 0.90, 0.23, 0.39, 0.94, and 0.81 eV, respectively, whereas D, CD_2, and CD bind to Ni_2^+ more strongly than to Co_2^+ by 0.69, 0.63, and 0.85 eV, respectively. Thus, the electronic structures of dimer species are a controlling element in these various bonds and, as previously discussed for iron cluster cations bonding to D atom, this can be explained by promotion energy arguments.[4] The Co_2^+ dimer has a configuration of $(4s\sigma_g)^2 d_A^8 d_B^7$,[77] which is formed by combining $Co^+(^3F, 3d^8)$ with $Co(^4F, 4s^2 3d^7)$. Fe_2^+ is believed to have a $(4s\sigma_g)^2 d_A^7 d_B^6$ electronic configuration,[4] and Ni_2^+ a $(4s\sigma_g)^2 d_A^9 d_B^8$ electronic configuration.[43] The general trend for C and CD_x binding to these three dimers is $Fe_2^+ < Co_2^+ < Ni_2^+$, except for Ni_2C^+ and $Ni_2CD_3^+$. One possible explanation for the general trend in bond energies is that the energy required to spin decouple the electrons needed for bonding increases from iron to cobalt to nickel because the number of unpaired spins involved increases from maxima of 7 [13 $3d$ electrons in ten molecular orbitals (MOs)] to 5 to 3, respectively. Clearly, *ab initio* calculations on such species would be very useful in understanding the details of these bond energies.

For $n=3$ and 4, iron, cobalt, and nickel cation cluster bond energies to D and CD_x species are very similar, which indicates that the effect of the electronic structure on binding D and CD_x species becomes smaller as the clusters get larger. Notable exceptions include the Co_3^+–CD_2 bond which is 0.80 eV stronger than Fe_3^+–CD_2 and ≥ 0.1 eV weaker than Ni_3^+–CD_2, a trend that presumably has a similar explanation as the dimers above. In contrast, the Co_4^+–CD bond is 0.44 eV stronger than both Fe_4^+–CD and Ni_4^+–CD, which suggests that the electron configuration of the cobalt tetramer cation is such that formation of three covalent bonds to CD is particularly facile.

The bond energies for D and CD_x to Co_n^+, Fe_n^+, and Ni_n^+ rapidly reach plateaus with increasing cluster size. For larger clusters, $n \geq 10$, the average bond energies for Co_n^+ to D, C, CD, and CD_2 (2.6 ± 0.1, 6.2 ± 0.1, 5.9 ± 0.1, and 4.5 ± 0.2 eV) are similar to the values of Fe_n^+ (Ni_n^+) D, C, CD, and CD_2, 2.6 ± 0.2 (2.6 ± 0.1), 6.1 ± 0.2 (6.5 ± 0.1), 5.9 ± 0.4 (5.9 ± 0.2), and 4.2 ± 0.4 ($\geq 3.9 \pm 0.1$ with a best estimate of 4.2 ± 0.4) eV, respectively. Clearly, D, C, CD, and CD_2 binding to cobalt, iron, and nickel metal clusters have the same bond orders (single, triple, triple, and double bonds, respectively). D and CD have very similar bond energies for all three metals, whereas the carbide (C) bond energies to nickel are slightly stronger than those to iron and cobalt, by 0.3–0.4 eV. This may simply be because Ni has more electrons than Fe and Co, which allows better donation to the empty p orbital on a C atom. Given these trends, Co_n^+ bonds to CD_2 are expected to be about the same or perhaps a little stronger than Fe_n^+ bonds to CD_2 for $n \geq 10$. This is true of the estimated values, 4.5 ± 0.2 eV, but would not be true of the bond energies derived directly from the thresholds for reactions (4), $>3.8 \pm 0.1$ eV, Table II.

C. Bond energies compared to bulk-phase values

In previous work, cluster studies appear to provide valuable information about thermochemistry for species bound to surfaces, especially molecular fragments. As noted in Sec. I, both Co_n^+–D and Co_n^+–O bond energies measured in our laboratory for larger clusters match bulk-phase values for these atomic adsorbates well. Similarly good agreement has been found for bond energies of D and O atoms binding to clusters of Fe_n^+,[4,5] Cr_n^+,[7,10] V_n^+,[9,12] and Ni_n^+ (Refs. 13–15) versus bulk-phase values. This correspondence indicates that chemical binding is largely a local phenomenon as long as clusters have enough electronic "flexibility" to form strong covalent bonds. This conclusion suggests that it is reasonable to use cluster models to study surface reactivities of transition metals.

In contrast to the atomic H and O systems, there is little experimental information on the thermochemistry of organic fragments (C, CH, CH_2, and CH_3) bound to cobalt surfaces. The successful comparison of surface chemisorption energies for H and O atoms to the bond energies for larger cluster ions suggests that our cluster thermochemistry can be used to estimate surface binding energies for these molecular fragments, as previously argued in our analogous work for CD_x ($x=0-3$) fragments binding to iron and nickel cluster cations.[11,26] Our recommended values, taken from the average values for clusters larger than nine cobalt atoms, are $D(Co_n^+-C)=6.23 \pm 0.13$ eV, $D(Co_n^+-CD)=5.92 \pm 0.14$ eV,

$D(Co_n^+-CD_2)=4.52\pm0.20(>3.82\pm0.09)$ eV, and $D(Co_n^+-CD_3)=2.59\pm0.10$ eV [assumed to equal the $D(Co_n^+-D)$ values].

The binding of C to nickel surfaces has been measured, but the only value available for cobalt surfaces is an estimate of 7.0 eV from the enthalpies of formation of cobalt-carbide compounds by Benziger.[21] Comparison to bulk-phase compounds appears to be a reasonable means to estimate adsorption enthalpies for oxides and nitrides, but insufficient data are available to assess its accuracy for carbides. This estimate is about 0.8 eV higher than our Co_n^+-C bond energies for larger clusters, comparable to the differences observed for the analogous data for iron and nickel.[11,26] One explanation for these differences is that the bulk-phase estimate includes contributions from interstitial tetracoordinate C, species that should not be accessible to surfaces or clusters. Certainly, the bond energy patterns noted above, specifically the agreement between our Co_n^+-C and Co_n^+-CD bond energies, indicate that cluster-carbides form triple bonds and are not tetracoordinate.

In the absence of experimental data for cobalt surfaces, our experimental estimates can be compared to theoretical values for surface binding energies. Burghgraef *et al.*[78] chose a one-layer 7-atom cluster and a spherical 13-atom cluster to model the cobalt surface and studied the adsorptions of C, CH, CH_2, CH_3, and H on these clusters using quasirelativistic calculations based on density functional theory. The main advantage of the seven-atom model is that it models a Co(111) and Co(0001) surface, but the small one-layer cluster suffers from boundary effects that can be reduced by adopting a spherical 13-atom cluster. Burghgraef *et al.* found that CH_3 prefers onefold sites, with calculated adsorption energies on Co_7 and Co_{13} of 1.09 and 2.09 eV, respectively. In contrast, H prefers a threefold site with adsorption energies of 2.48 and 2.80 eV on Co_7 and Co_{13}, respectively. Likewise, CH_2, CH, and C prefer threefold sites with adsorption energies of 3.74, 6.07, and 6.48 eV on Co_7 and 4.11, 5.85, and 6.58 eV on Co_{13}, respectively. Note that all fragments except CH adsorb more strongly on the 13-atom cluster than on a 7-atom cluster. The adsorption energies of Co_{13} to CH_2, CH, C, and H are 4.11, 5.85, 6.58, and 2.80 eV, respectively, which compare nicely with our values for larger clusters, 4.52, 5.92, 6.23, and 2.59 eV. However, these calculations suggest that because the binding geometry of the spherical H atom differs from that of the more directional CH_3 group, H atoms bind more tightly to cobalt surfaces than CH_3 groups by 0.4–0.7 eV.

Zheng *et al.*[79] used extended Hückel methods to calculate bonding energies for CH_x adsorption on a two-dimensional slab designed to model Co(0001). For CH_3, they obtain adsorption energies of 3.73 eV for a onefold site, 2.64 eV for a twofold site, and 2.36 eV for a threefold site. Although the site preference agrees with the results of Burghgraef *et al.*, the adsorption energy is much higher than those theoretical results. For CH_2, Zheng *et al.* found a preference for a twofold site with an adsorption energy of 6.35 eV, followed by 6.32 eV for a onefold site and 5.75 eV for a threefold site. These values are much higher than the theoretical results of Burghgraef *et al.* as well as our experimental bond energies and have a different site preference than found by Burghgraef *et al.* For CH, Zheng *et al.* calculated a preference for a threefold site with an adsorption energy of 9.36 eV, followed by a twofold site at 9.04 eV and a onefold site at 8.84 eV. Again these adsorption energies are much higher than those of Burghgraef *et al.* and our experimental results.

Klinke *et al.*[80–82] used density functional theory within the generalized gradient approximation and the full-potential linear augmented planewave method, which is designed to simulate the extended surface. For low coverages (0.5 monolayer) of hydrogen atoms, they find bond energies of 2.67, 2.90, and 2.89 eV for bridging, fcc hollow, and hcp hollow sites, respectively.[80] The latter are 12% greater than the experimental results of 2.60 eV,[18,19] which agree well with our cluster results of 2.59 eV.[17] For low coverages (0.25 monolayer) of carbon atoms, this approach finds bond energies of 6.21, 6.88, and 7.05 eV for bridging, fcc hollow, and hcp hollow sites, respectively.[81] The former value agrees well with our experimental results of 6.23 ± 0.13 eV, whereas the latter are 10%–13% higher. For low coverages (0.25 monolayer) of methylidyne (CH), they find that the hollow sites of fcc and hcp Co(0001) surfaces have binding energies of 6.57 and 6.68 eV, respectively,[82] which again are 11%–13% higher than our experimental estimate of 5.92 ± 0.14 eV. Note, however, that the relative differences between the H, C, and CH binding energies are comparable between experiment and this level of theory. Notably these authors used their calculated results in a global model of FT chemistry to good effect.[83]

D. Reaction mechanism

To understand the mechanism of the reactions of cobalt cluster cations with methane, we re-examine what is known about the reactions of atomic Co^+ ions with CD_4 (Ref. 49) because the basic principles involved should be the same and have proven useful in our $Fe_n^+ + CD_4$ (Ref. 11) and $Ni_n^+ + CD_4$ studies.[26] The reaction of atomic Co^+ with CD_4 occurs by C–D bond activation to form a $D-Co^+-CD_3$ intermediate. At low energies, the most favorable reaction is dehydrogenation to form $CoCD_2^+ + D_2$, which involves rearrangement of the $D-Co^+-CD_3$ intermediate to a four-centered TS involving an incipient D-D bond. The energy of this TS has been measured to lie 0.35 ± 0.08 eV above the $CoCD_2^+ + D_2$ product asymptote.[49] At high energies, the $D-Co^+-CD_3$ molecule decomposes by simple Co–C bond cleavage to form $CoD^+ + CD_3$. Competing with this is the cleavage of the Co–D bond to yield $CoCD_3^+ + D$. The former reaction is favored because of conservation of angular momentum effects.[84] These simple bond cleavage reactions involve only loose TSs, while that for dehydrogenation involves more complicated rearrangement over the tight four-centered TS.

The electronic requirements for sigma bond activation of CD_4 at a transition metal center can be viewed fairly simply. In order to break the C–D covalent bond and simultaneously form two new bonds between the metal and the D and CD_3 fragments, the metal center must accept electron density from the C–D bond and donate electron density into the an-

tibonding orbital of this bond. Formally, this is an oxidative addition process in which the metal oxidation state increases by 2, although neither the D nor CD_3 ligand carries a full negative charge. For atomic first row transition metal ions, the acceptor orbital is largely the $4s$ orbital, and the donor is a $3d\pi$. Combining these orbitals with the bonding and antibonding σ orbitals of the C–D bond leads to pairs of bonding and antibonding MOs for the $D-Co^+-CD_3$ intermediate. To create the most favorable bonding situation, four electrons are needed to occupy the bonding MOs with no additional electrons for the antibonding MOs. As the C–D bond provides two electrons, the most efficient reaction is expected when the metal has an empty σ-acceptor and a doubly occupied π-donor.

In analogy with the mechanism for reaction of the monomer with methane, the first step in the reaction of the cobalt cluster cations with CD_4 is C–D bond activation to form a $D-Co_n^+-CD_3$ intermediate. The observation of $Co_nCD_4^+$ products for $n>9$ that can be assigned to chemisorbed intermediates is clearly consistent with this hypothesis. The overall thermodynamics for forming the $D-Co^+-CD_3$ intermediates can be estimated by simple bond additivity as equal to $D(D-CD_3)-2D(Co_n^+-D)$, where we assume $D(Co_n^+-CD_3) \approx D(Co_n^+-D)$. This estimate assumes that binding D to the cluster does not affect the binding of CD_3 to the cluster and vice versa. This assumption seems reasonable for larger clusters because each ligand can find a binding site remote from the other ligand. This bond additivity estimate suggests that formation of $D-Co^+-CD_3$ is exothermic for $n=2$ and $n>8$ and endothermic by an average of 0.3 ± 0.1 eV for $n=1$ and 3–8. Thus, the thresholds observed for formation of $D-Co^+-CD_3$ ($n>9$), measured to be 1.0 ± 0.1 eV, can be attributed to barriers for $D-CD_3$ bond activation.

Co_nD^+ is the major ionic product observed at higher energies and can be formed by cleaving the Co–C bond in a $D-Co_n^+-CD_3$ intermediate to eliminate an intact methyl group. Once the Co_nD^+ product begins to be formed, the cross sections for $Co_nCD_2^+$ and Co_nC^+ products formed at lower energies begin to decline, Figs. 1–5, indicating competition between these channels. Such competition is also indicated by the fact that our modeling of the data needs to include competition between reactions (1) and (4) in order to obtain accurate Co_nD^+ bond energies. Such competition is clearly consistent with all reaction channels sharing the putative $D-Co_n^+-CD_3$ species as a common intermediate.

The formation of Co_2D^+ and $Co_2CD_3^+$ in the dimer system must occur by simple bond cleavage from the $D-Co_2^+-CD_3$ intermediate, similar to the mechanism for reaction of the monomer with methane.[49] Unlike the monomer and dimer, $Co_nCD_3^+$ products are not observed for larger cobalt clusters. This is likely to be a matter of experimental sensitivity combined with the fact that formation of this product is inhibited by angular momentum conservation considerations.[84] The reduced mass of the $Co_n^+ + CD_4$ reactants (about 20 amu) is similar to that for the $Co_nD^+ + CD_3$ product channel (about18 amu), whereas the reduced mass of the $Co_nCD_3^+ + D$ product channel is much lower (about 2 amu). Consequently, the phase space available to the $Co_nCD_3^+ + D$ product channel is much smaller than that associated with the $Co_nD^+ + CD_3$. For the dimer and trimer cobalt cations, small cross sections for formation of secondary methyl products ($CoCD_3^+ + CoD$ and $Co_2CD_3^+ + CoD$) are observed. The thermochemistry demonstrates that the formation of these $Co_{n-1}CD_3^+$ products as well as the secondary $Co_{n-1}CD^+$ products is concomitant with neutral CoD. These observations provide direct evidence that C–D bond activation by metal clusters produces an intermediate where the D and CD_3 ligands are bound to different cobalt atoms, i.e., $DCo-Co_{n-1}CD_3^+$.

The barrier to the dehydrogenation reaction of the monomer cation ($Co^+ + CD_4 \rightarrow CoCD_2^+ + D_2$) is associated with a four-centered TS lying in the exit channel 0.35 ± 0.08 eV above the energy of the products.[49] For reaction of the dimer and trimer, dehydrogenation is also found to have a barrier, which lies 0.7 ± 0.2 eV above the $Co_nCD_2^+ + D_2$ products. This barrier could again correspond to a four-centered elimination from an intermediate in which both ligands are attached to the same cobalt atom. However, another possibility is that this reaction occurs by a five-centered elimination from a $DCo-Co_{n-1}CD_3^+$ intermediate, whose existence is suggested by the observations noted in the previous paragraph. Complicating factors in thinking about the likely pathway is whether any of the ligands, D, CD_2, or CD_3, are bridging rather than terminal. Without other information, no definitive conclusions regarding the mechanism of the dehydrogenation process by the cobalt dimer and trimer cation can be made.

For larger cluster cations, $n\geq3$, the secondary dehydrogenation reactions (9) were not observed, hence the presence of barriers possibly inhibiting reactions (4) cannot be measured directly. However, barriers in excess of the endothermicities were observed for dehydrogenation reactions of methane by the larger clusters of Fe_n^+ (Ref. 11) and were also surmised for the analogous reactions with Ni_n^+.[26] These barriers were assigned to lie in the entrance channel (C–D activation step) rather than in the exit channel. The thresholds measured for $Co_nCD_2^+$ ($n=4-16$) formation do not vary appreciably (average of 1.15 ± 0.18 eV, Tables S4–S16), although they do decline slightly with increasing cluster size. Overall, these comparisons suggest that the thresholds measured here for reactions (4) correspond to barriers for C–D activation in the entrance channel, rather than the thermodynamic limits for $Co_nCD_2^+$ formation. Hence bond energies derived from these thresholds are lower limits to the true thermochemistry for $Co_nCD_2^+$. In analogy to the measured barriers for Co^+, Co_2^+, and Co_3^+, the barriers in excess of the endothermicities for the dehydrogenation reaction (4) of larger clusters are estimated as 0.7 ± 0.2 eV above. This value also corresponds nicely to the barriers in the analogous reaction directly measured for the larger clusters of Fe_n^+.[11]

Reactions of larger clusters presumably have the same complicated mechanistic possibilities mentioned above for Co_2^+. In addition, $(CoD)(CoD)(Co_{n-2}CD_2)^+$ intermediates formed by the migration of two D atoms from the methane to separate cobalt atoms and possible bridging ligands might also be considered. This kind of intermediate is clearly not possible for smaller clusters. Thus, dehydrogenation can occur remotely from the $Co_n^+-CD_2$ bond, as also suggested in

the iron and nickel system,[11,26] which can explain why the barrier in the exit channel observed for $n=1$ might no longer be rate limiting for larger clusters. In general, the dehydrogenation reaction (4) to form $Co_nCD_2^+$ products becomes more facile with increasing cluster size although there is a minimum in the observed reactivity at $n=6$. Likewise, the double dehydrogenation reaction (2) to form Co_nC^+, which *must* occur via a $Co_nCD_2^+$ transient intermediate, follows the same trend. For the largest clusters, the double dehydrogenation reactions to form Co_nC^+ are sufficiently facile that these cross sections become much larger than those of $Co_nCD_2^+$.

VI. CONCLUSION

In this work, we use a guided ion beam tandem mass spectrometer to examine the kinetic energy dependences of the reactions of size-specific cobalt cluster cations ($n=2-16$) with deuterated methane. We report cross sections for six to ten reactions for each cluster system, all of which exhibit thresholds. The main reactions observed are the dehydrogenation reactions (4), double dehydrogenation reactions (2), and loss of CD_3 reactions (1) to form $Co_nCD_2^+$, Co_nC^+, and Co_nD^+, respectively. Our analysis of the cross sections yields two independent values for the bond energies for most clusters to D, C, and CD through the energy dependence of both primary and secondary routes to the various products, but only the primary pathway is observed for $Co_nCD_2^+$ formation, except for $n=2-4$. For D (where there are also literature values available[17]), C, and CD, the multiple values obtained are in good agreement with one another, whereas for the case of CD_2, the secondary thresholds obtained for reactions of $n=2-4$ yield bond energies for $(n-1)=1-3$ exceeding those obtained from the primary thresholds of reactions (4). This is evidence that there are barriers of about 0.7 ± 0.2 eV in excess of the endothermicity of the initial dehydrogenation reaction for $n=2-4$. We estimate that the true thermodynamic bond energies for $Co_nCD_2^+$ can be estimated by adding this 0.7 ± 0.2 eV barrier to the bond energies extracted from modeling the cross sections for reactions (4). For larger clusters, these barriers are believed to lie in the initial dissociative chemisorption steps, in analogy with the results found for iron cluster cations.[11]

Best estimates for C, CD, CD_2, and CD_3 binding energies to cationic cobalt clusters are obtained from analyses of the reaction cross sections. The relative magnitudes in the D, C, CD, CD_2, and CD_3 bond energies to the cobalt cluster cations are consistent with simple bond order considerations: Single, triple, triple, double, and single bond orders, respectively. Comparison of these values to limited experimental information for binding of D and O atoms to surfaces suggests that our experimental bond energies for larger clusters provide reasonable estimates for heats of adsorption to cobalt surfaces. As limited experimental information is available for molecular species binding to surfaces, the thermochemistry derived here for cobalt clusters bound to C, CD, CD_2, and possibly CD_3 (using D as a model) provides the first experimental thermodynamic information on such molecular species. These values are in reasonable agreement with the theoretical estimates for C, CD, and CD_2 binding to cluster models of Co surfaces obtained by Burghgraef *et al.*[78]

ACKNOWLEDGMENTS

This work is supported by the Chemical Sciences, Geosciences, and Biosciences Division, Office of Basic Energy Sciences, Office of Science, U.S. Department of Energy DE-FG02-03ER15404.

[1] P. B. Armentrout, J. B. Griffin, and J. Conceicao, in *Progress in Physics of Clusters*, edited by G. N. Chuev, V. D. Lakino, and A. P. Nefedov (World Scientific, Singapore, 1999), p. 198.
[2] P. B. Armentrout, Annu. Rev. Phys. Chem. **52**, 423 (2001).
[3] P. B. Armentrout, Eur. J. Mass Spectrom. **9**, 531 (2003).
[4] J. Conceicao, S. K. Loh, L. Lian, and P. B. Armentrout, J. Chem. Phys. **104**, 3976 (1996).
[5] J. B. Griffin and P. B. Armentrout, J. Chem. Phys. **106**, 4448 (1997).
[6] J. B. Griffin and P. B. Armentrout, J. Chem. Phys. **107**, 5345 (1997).
[7] J. B. Griffin and P. B. Armentrout, J. Chem. Phys. **108**, 8062 (1998).
[8] J. B. Griffin and P. B. Armentrout, J. Chem. Phys. **108**, 8075 (1998).
[9] J. Xu, M. T. Rodgers, J. B. Griffin, and P. B. Armentrout, J. Chem. Phys. **108**, 9339 (1998).
[10] J. Conceicao, R. Liyanage, and P. B. Armentrout, Chem. Phys. **262**, 115 (2000).
[11] R. Liyanage, X. G. Zhang, and P. B. Armentrout, J. Chem. Phys. **115**, 9747 (2001).
[12] R. Liyanage, J. Conceicao, and P. B. Armentrout, J. Chem. Phys. **116**, 936 (2002).
[13] F. Y. Liu, R. Liyanage, and P. B. Armentrout, J. Chem. Phys. **117**, 132 (2002).
[14] K. Koszinowski, D. Schroder, H. Schwarz, R. Liyanage, and P. B. Armentrout, J. Chem. Phys. **117**, 10039 (2002).
[15] D. Vardhan, R. Liyanage, and P. B. Armentrout, J. Chem. Phys. **119**, 4166 (2003).
[16] R. Liyanage, J. B. Griffin, and P. B. Armentrout, J. Chem. Phys. **119**, 8979 (2003).
[17] F. Y. Liu and P. B. Armentrout, J. Chem. Phys. **122**, 194320 (2005).
[18] K. Christmann, Surf. Sci. Rep. **9**, 1 (1988).
[19] M. E. Bridge, C. M. Comrie, and R. M. Lambert, J. Catal. **58**, 28 (1979).
[20] K. H. Ernst, E. Schwarz, and K. Christmann, J. Chem. Phys. **101**, 5388 (1994).
[21] J. B. Benziger, in *Metal-Surface Reaction Energetics*, edited by E. Shustorovich (VCH, New York, 1991), p. 53.
[22] I. Toyoshima and G. A. Somorjai, Cat. Rev. - Sci. Eng. **19**, 105 (1979).
[23] C. N. R. Rao, P. V. Kamath, and S. Yashonath, Chem. Phys. Lett. **88**, 13 (1982).
[24] V. E. Ostrovskii, Russ. J. Phys. Chem. **62**, 330 (1988).
[25] F. Y. Liu, F. X. Li, and P. B. Armentrout, J. Chem. Phys. **123**, 064304 (2005).
[26] F. Y. Liu, X. G. Zhang, R. Liyanage, and P. B. Armentrout, J. Chem. Phys. **121**, 10976 (2004).
[27] P. E. M. Siegbahn and U. Wahlgren, in *Metal-Surface Reaction Energetics*, edited by E. Shustorovich (VHC, New York, 1991), p. 1.
[28] H. Schulz, Appl. Catal., A **186**, 3 (1999).
[29] S. J. Jenkins and D. A. King, J. Am. Chem. Soc. **122**, 10610 (2000).
[30] M. E. Dry, Catal. Today **71**, 227 (2002).
[31] M. L. Turner, N. Marsih, B. E. Mann, R. Quyoum, H. C. Long, and P. M. Maitlis, J. Am. Chem. Soc. **124**, 10456 (2002).
[32] Z. P. Liu and P. Hu, J. Am. Chem. Soc. **124**, 11568 (2002).
[33] J. J. C. Geerlings, M. C. Zonnevylle, and C. P. M. de Groot, Surf. Sci. **241**, 315 (1991).
[34] B. G. Johnson, C. H. Bartholomew, and D. W. Goodman, J. Catal. **128**, 231 (1991).
[35] P. K. Agrawal, J. R. Katzer, and W. H. Manogue, Ind. Eng. Chem. **21**, 385 (1982).
[36] P. K. Agrawal, J. R. Katzer, and W. H. Manogue, J. Catal. **69**, 312 (1981).
[37] M. A. Vannice, J. Catal. **37**, 449 (1975).
[38] W. H. Lee and C. H. Bartholomew, J. Catal. **120**, 256 (1989).
[39] J. Lahtinen, T. Anraku, and G. A. Somorjai, J. Catal. **142**, 206 (1993).
[40] S. K. Loh, D. A. Hales, L. Lian, and P. B. Armentrout, J. Chem. Phys. **90**, 5466 (1989).

[41] D. A. Hales, C.-X. Su, L. Lian, and P. B. Armentrout, J. Chem. Phys. **100**, 1049 (1994).
[42] C.-X. Su and P. B. Armentrout, J. Chem. Phys. **99**, 6506 (1993).
[43] L. Lian, C.-X. Su, and P. B. Armentrout, J. Chem. Phys. **96**, 7542 (1992).
[44] E. Teloy and D. Gerlich, Chem. Phys. **4**, 417 (1974).
[45] D. Gerlich, Adv. Chem. Phys. **82**, 1 (1992).
[46] N. R. Daly, Rev. Sci. Instrum. **31**, 264 (1960).
[47] K. M. Ervin and P. B. Armentrout, J. Chem. Phys. **83**, 166 (1985).
[48] See EPAPS Document No. E-JCPSA6-130-009906 for 14 figures and 16 tables. For more information on EPAPS, see http://www.aip.org/pubservs/epaps.html.
[49] C. L. Haynes, Y.-M. Chen, and P. B. Armentrout, J. Phys. Chem. **99**, 9110 (1995).
[50] A. Nakajima, T. Kishi, Y. Sone, S. Nonose, and K. Kaya, Z. Phys. D: At., Mol. Clusters **19**, 385 (1991).
[51] A. A. Shvartsburg, K. M. Ervin, and J. H. Frederick, J. Chem. Phys. **104**, 8458 (1996).
[52] R. J. Birgeneau, J. Cordes, G. Dolling, and A. D. B. Woods, Phys. Rev. **136**, A1359 (1964).
[53] G. Simmons and H. Wang, *Single Crystal Elastic Constants and Calculated Aggregate Properties: A Handbook*, 2nd ed. (MIT., Cambridge, 1971).
[54] N. W. Ashcroft and N. D. Mermin, *Solid State Physics* (Saunders College, Philadelphia, 1976), p. 461.
[55] R. Rohlsberger, W. Sturhahn, T. S. Toellner, K. W. Quast, P. Hession, M. Hu, J. Sutter, and E. E. Alp, J. Appl. Phys. **86**, 584 (1999).
[56] T. Shimanouch, *Table of Molecular Vibrational Frequencies, Consolidated* (National Bureau of Standards, Washington, DC, 1972).
[57] P. B. Armentrout, Int. J. Mass Spectrom. **200**, 219 (2000).
[58] K. M. Ervin, Chem. Rev. **101**, 391 (2001).
[59] P. B. Armentrout, J. Am. Soc. Mass Spectrom. **13**, 419 (2002).
[60] R. G. Gilbert and S. C. Smith, *Theory of Unimolecular and Recombination Reactions* (Blackwell Scientific, Oxford, 1990).
[61] K. A. Holbrook, M. J. Pilling, and S. H. Robertson, *Unimolecular Reactions*, 2nd ed. (Wiley, New York, 1996).
[62] D. G. Truhlar, B. C. Garrett, and S. J. Klippenstein, J. Phys. Chem. **100**, 12771 (1996).
[63] M. T. Rodgers, K. M. Ervin, and P. B. Armentrout, J. Chem. Phys. **106**, 4499 (1997).
[64] W. E. Billups, S.-C. Chang, R. H. Hauge, and J. L. Margrave, J. Am. Chem. Soc. **117**, 1387 (1995).
[65] M. E. Jacox, in J. Phys. Chem. Ref. Data Monogr. **3**, 3 (1994).
[66] D. G. Musaev, K. Morokuma, N. Koga, K. A. Nguyen, M. S. Gordon, and T. R. Cundari, J. Phys. Chem. **97**, 11435 (1993).
[67] V. A. Spasov, T. H. Lee, J. P. Maberry, and K. M. Ervin, J. Chem. Phys. **110**, 5208 (1999).
[68] Co–D and Co–CD_3 bond energies have been adjusted from Co–H and Co–CH_3 bond energies (Ref. 49) by considering the differences in zero point energies.
[69] Thermochemistry for deuterated fragments of CD_4 is compiled in Ref. 70.
[70] C. L. Haynes, Y. M. Chen, and P. B. Armentrout, J. Phys. Chem. **100**, 111 (1996).
[71] M. T. Rodgers and P. B. Armentrout, J. Chem. Phys. **109**, 1787 (1998).
[72] P. B. Armentrout and B. L. Kickel, in *Organometallic Ion Chemistry*, edited by B. S. Freiser (Kluwer Academic, Dordrecht, 1996), p. 1.
[73] C. L. Haynes and P. B. Armentrout, Organometallics **13**, 3480 (1994).
[74] K. P. Huber and G. Herzberg, *Molecular Spectra and Molecular Structure. IV. Constants of Diatomic Molecules* (Van Nostrand Reinhold, New York, 1979).
[75] P. B. Armentrout, L. S. Sunderlin, and E. R. Fisher, Inorg. Chem. **28**, 4436 (1989).
[76] M. R. Albert and J. T. Yates, *The Surface Scientist's Guide to Organometallic Chemistry* (American Chemical Society, Washington, DC, 1987).
[77] D. A. Hales and P. B. Armentrout, J. Cluster Sci. **1**, 127 (1990).
[78] H. Burghgraef, A. P. J. Jansen, and R. A. van Santen, Surf. Sci. **324**, 345 (1995).
[79] C. Zheng, Y. Apeloig, and R. Hoffmann, J. Am. Chem. Soc. **110**, 749 (1988).
[80] D. J. Klinke and L. J. Broadbelt, Surf. Sci. **429**, 169 (1999).
[81] D. J. Klinke, S. Wilke, and L. J. Broadbelt, J. Catal. **178**, 540 (1998).
[82] D. J. Klinke, D. J. Dooling, and L. J. Broadbelt, Surf. Sci. **425**, 334 (1999).
[83] D. J. Klinke and L. J. Broadbelt, Chem. Eng. Sci. **54**, 3379 (1999).
[84] R. H. Schultz, J. L. Elkind, and P. B. Armentrout, J. Am. Chem. Soc. **110**, 411 (1988).
[85] J. L. Elkind and P. B. Armentrout, J. Phys. Chem. **90**, 6576 (1986).